

THE CATHOLIC UNIVERSITY OF AMERICA

Selection and Analysis of HIV-1 Envelope Epitopes for Design of Vaccines that can  
Induce Broadly Neutralizing Antibodies

A DISSERTATION

Submitted to the Faculty of the

Department of Biology

School of Arts and Sciences

Of The Catholic University of America

In Partial Fulfillment of the Requirements

For the Degree

Doctor of Philosophy

By

Lindsay Wiczorek

Washington, D.C.

2012

Selection and Analysis of HIV-1 Envelope Epitopes for Design of Vaccines that can  
Induce Broadly Neutralizing Antibodies

Lindsay Wiczorek, Ph.D.

Director: Venigalla B. Rao, Ph.D.

HIV-1 vaccines are designed to mimic the structure and contextual elements of viral epitopes that have the potential to induce broadly neutralizing antibodies (bnAbs) *in vivo*. The structure of gp41 membrane proximal external region (MPER), targeted by three bnAbs, is poorly defined. The goal of this study is to select epitopes with enhanced binding to MPER bnAbs, to identify neutralization-competent structures by characterizing the function of epitope-specific antibodies *in vivo* and to determine if these selected MPER epitopes can be used to broaden the immune response as potential vaccines.

MPER epitopes were selected by biopanning with phage-displayed peptide libraries against bnAbs 4E10, 2F5 and Z13. Epitopes were screened in antigen competition binding assays where M13-displayed epitopes competed with HIV-1 envelope peptides or infectious HIV-1 particles for antibody binding. *In vivo* response to MPER was assessed by M13 immunoprecipitation and neutralization competition assays using HIV+ plasma. Immunogenicity of select epitopes was determined by immunization of mice and elicited cellular and humoral immune responses were assessed.

Unique 4E10, and known 2F5 and Z13, epitopes were selected from M13 phage display libraries, which were able to compete with envelope peptide and HIV-1 for antibody binding. 4E10 and 2F5 epitopes were found to be immunogenic during HIV-1 infection; of the twelve HIV+ patient plasma tested, 100% and 58% reacted with phage-

displayed 4E10 and 2F5 MPER epitopes, respectively. 4E10-epitopes were capable of absorbing MPER-specific neutralizing antibodies in HIV+ plasma. Mouse immunization with selected, neutralization-competent MPER epitopes elicited HIV-1 specific cellular and humoral immune responses and boosted the neutralizing activity of a gp145 protein subunit vaccine.

Unique 4E10 epitopes, that represent functional HIV-1 envelope trimers, were identified. Chronically HIV-infected individuals generate neutralizing antibodies to a subset of the selected MPER-variant epitopes. These M13-displayed 4E10 epitopes have the potential to elicit HIV-1 neutralizing antibodies in mice. Increasing the range of antibody recognition to MPER, potentially by vaccination with multiple MPER variant epitopes, will be the key to improve HIV-1 vaccine design.

This dissertation by Lindsay Wieczorek fulfills the dissertation requirement for the doctoral degree in biology approved by Venigalla B. Rao, Ph.D., as Director, and by John E. Golin, Ph.D., James J. Greene, Ph.D. and Victoria R. Polonis, Ph.D. as Readers.

---

Venigalla B. Rao, Ph.D., Director

---

John E. Golin, Ph.D., Reader

---

James J. Greene, Ph.D., Reader

---

Victoria R. Polonis, Ph.D., Reader



## TABLE OF CONTENTS

	Page
List of Figures	iv
List of Tables	vi
Acknowledgements	vii
Introduction	1
Materials and Methods	15
Experimental Results	36
Discussion	71
References	80

## LIST OF FIGURES

Figure	Page
1. The schematic structure HIV-1 gp160, gp120 and gp41	2
2. Structure of HIV-1 and location of bnAb binding sites	3
3. Schematic of HIV-1 cellular entry and target epitopes for bnAbs	4
4. Diagram of gp41 highlighting bnAb epitopes in MPER	8
5. Representation of MPER orientation changes induced by bnAb binding	9
6. Schematic of MPER bnAb epitopes on functional HIV-1 spike	10
7. Diagram of phage display biopanning procedure	22
8. Neutralization profile of four bnAbs	37
9. 2F5 mutations in neutralization sensitive and resistant isolates	39
10. 2F5 and 4E10 capture of HIV-1 and sCD4-bound HIV-1	41
11. Neutralization profile of 12 HIV-positive patient plasma samples	42
12. Alignment of 4E10-selected Ph.D.-12 sequences	46
13. MPER homology of bnAb selected epitopes	48
14. Number of MPER homologous amino acids per selected epitope	49
15. Effect of HIV-1 competition on 4E10 epitope selection	50
16. ELISA binding curves and binding titers for bnAb-selected epitopes	52
17. MPER peptide inhibition curves and IC <sub>50</sub> s for bnAb-selected epitopes	54
18. HIV-1 capture competition and effect of sCD4-binding	55
19. Correlation between relative binding affinity and binding competition	56
20. Detection of MPER epitope-specific IgG in HIV-positive plasma	59

21. Trends in MPER-specific IgG and neutralization breadth and potency	61
22. Inhibition of MPER-specific neutralization by plasma screens	62
23. Inhibition of MPER-specific neutralization by plasma titers	63
24. Cellular immunogenicity characterized by INF $\gamma$ ELISPOT	66
25. Cellular immunogenicity characterized by IL-2 intracellular staining	67
26. Humoral immunogenicity characterized by binding ELISA	69
27. Humoral immunogenicity characterized by neutralization assay	70

## LIST OF TABLES

Table	Page
1. Multi-subtype panel of HIV-1 isolates	16
2. Mouse immunization scheme	31
3. MPER sequence variability	38
4. M13 recovery after consecutive rounds of biopanning	44
5. Unique 2F5, Z13 and 4E10 sequences selected by bnAb biopanning	45
6. M13-displayed epitopes selected for further analysis	51
7. Predicted secondary and tertiary structure of M13-displayed epitopes	58

## ACKNOWLEDGEMENTS

I would like to thank the many people that supported me in the completion of this project. I am indebted to my CUA advisor, Dr. Venigalla Rao, and my MHRP advisor, Dr. Vicky Polonis, whose guidance and support made this work possible. I would also like to thank my additional committee members, Dr. John Golin and Dr. James Greene, for their time and advice.

I want to acknowledge and thank everyone that contributed to this research. Dr. Bonnie Draper guided me through the structural modeling efforts. Dr. Mangala Rao, Dr. Tina Peachman, Dr. Nick Steers, Dr. Erik Billings, Sarah McCormack and Elaine Morrison played critical roles in the design, execution and analysis of the immunogenicity study. Maggie Wesberry, Sebastian Molnar and Brittani Barrows provided friendship and daily support in the Humoral Immunology Laboratory.

I would like to thank my family, John and Pat Wiczorek, Sarah and Phil Thoreson, and Andrew and Oliver Rosa Borges, for their constant support, understanding and encouragement.

## **Introduction**

### **HIV-1 epidemic**

HIV has infected more than 60 million people; roughly half of those have died from AIDS-related causes [1]. In the 30 years since its discovery, HIV has spread to every corner of the globe, devastating countries where infection rates are as high as 25% [2]. Interventions such as education, microbicide and drug therapy have been successful in reducing transmission but these alone will not be enough to end the pandemic [3]. A globally efficacious HIV vaccine is required. Induction of broadly neutralizing antibodies (bnAbs) is one of the ultimate goals in the development of a preventative HIV-1 vaccine [4,5,6,7].

### **HIV-1 envelope structure and function**

HIV-1 is an enveloped retrovirus that infects human CD4<sup>+</sup> T cells. Viral particles contain two surface-exposed viral proteins, gp120 and gp41; the remaining surface molecules are host cell-derived [8]. Gp120 and gp41, encoded by the *env* gene, are produced as a precursor protein, gp160 that is cleaved to produce mature viral proteins. Gp120, the surface domain that attaches the virus to the host cell, contains five constant regions separated by five variable loops [9]. Gp41, a class I viral fusion protein, contains a fusion peptide (FP), N- and C-heptad repeats (NHR and CHR) separated by an immunodominant loop, a pre-transmembrane domain (pre-TM) containing the membrane proximal external region (MPER), a transmembrane domain (TMD) and cytoplamic tail or endodomain (Figure 1) [10,11].

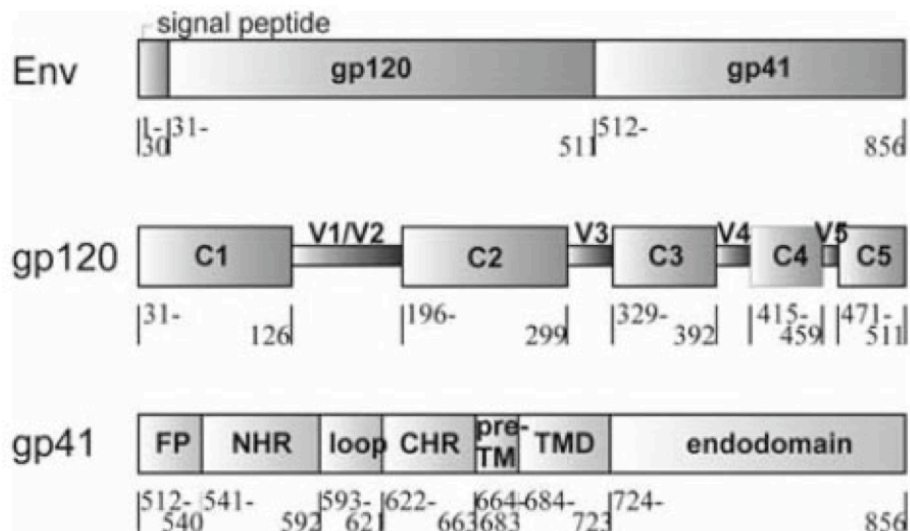


Figure 1. Schematic representation of the gp160 Env protein that is cleaved to produce mature gp120 and gp41 protein [11].

In the mature HIV-1 virion, gp120 and gp41 are non-covalently associated to form a trimeric spike in which the gp120 subunits, prominently displayed on the surface, are anchored by the transmembrane gp41 subunits (Figure 2) [12]. Gp120 and gp41 are the major target of the immune system and are subject to immunological pressure shortly after infection. Immune pressure and a high rate of error-prone replication allow for rapid sequence diversification in these two proteins, ensuring that some of the progeny viruses can continue to infect cells effectively [13]. Mutation, along with recombination, have produced enormous genetic diversity within and between HIV-1 subtypes [14].

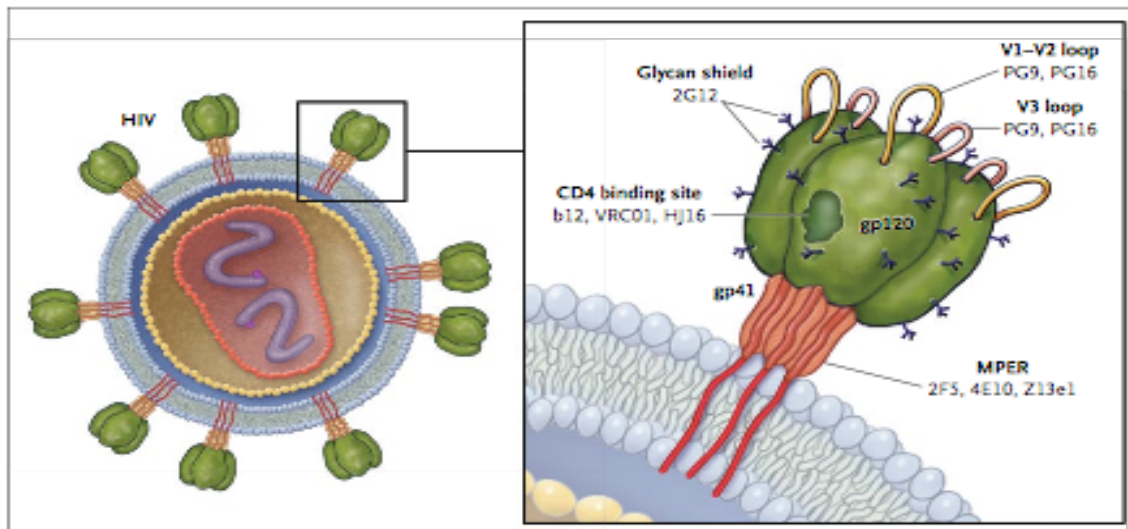


Figure 2. Schematic of HIV-1 structure and location of bnAbs binding sites: the CD4 binding site (b12, VRC01, HJ16) on gp120, the MPER (2F5, 4E10, Z13e1) of gp41, the glycan shield mannose clusters (2G12), and epitopes that reside in the variable loops 1, 2, and 3 on gp120 (PG9, PG16) [12].

Cellular infection, a process of viral attachment and fusion, is dynamic and requires significant structural rearrangement of the viral spike (Figure 3) [15]. Gp120 binds first to the CD4 receptor, then to a coreceptor, CCR5 or CXCR4. Initial CD4 binding induces a large conformational change in the envelope that exposes the previously occluded coreceptor binding site. Coreceptor binding induces another large conformational change that triggers the insertion of the gp41 fusion peptide into the host cell membrane, restructuring gp41 into the pre-hairpin intermediate state. Next, the NHR and CHR collapse bringing the gp41 fusion peptide and the MPER, associated with the host and viral membranes respectively, in proximity for fusion. The post-fusion gp41 six-helical bundle remains on the surface of the infected cell. During the transition to complete membrane fusion, gp41 assumes at least three fluid conformations: the pre-



fusion native state, a pre-hairpin intermediate state in which gp41 acts as a bridge between viral and cellular membranes, and the post-fusion hairpin state [15].

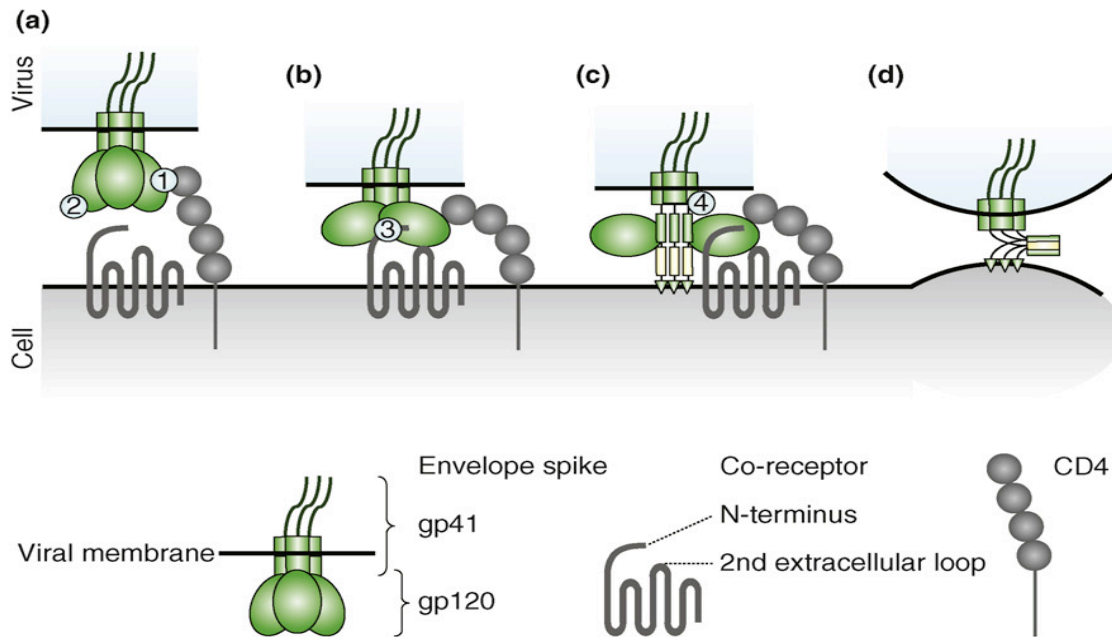


Figure 3. Schematic of HIV-1 cellular entry and target epitopes for bnAbs. (a) gp120 binds to CD4, (b) gp120 binds to the coreceptor, (c) gp41 fusion domain inserts into the target cell membrane. (d) gp41 changes conformation resulting in fusion of the target cell and viral membranes (gp120 not shown). Numbers in circles represent bnAb epitopes: (1) CD4 binding site (b12); (2) mannose cluster (2G12); (3) CD4-induced epitope (e.g. 17b); (4) membrane-proximal external region (2F5, Z13 4E10) [15].

Antibody binding to HIV-1 envelope can interrupt the viral infection process [16].

BnAbs are unique in that they target regions of HIV-1 that are highly conserved between viral strains and are required for successful infection. Mutations that prevent antibody interaction with these epitopes will produce viral particles that are not functional [17]. To date, very few bnAbs have been identified.

BnAbs that target gp120 bind either in the native state, preventing envelope interaction with host cell molecules such as CD4, or in the CD4-bound state, preventing

interaction with coreceptor or inhibiting the conformational changes required for infection [18,19,20]. BnAbs against gp120 include: b12, VRC01 and HJ16 which bind to the CD4-binding site, 2G12 which binds to the glycan shield mannose clusters, and pg9 and pg16 which binds to the variable loops. BnAbs that target the linear MPER of gp41, 4E10, 2F5 and Z13, bind to the native or pre-hairpin intermediate states and prevent conformational changes required for fusion (Figure 2) [19,21]. These MPER antibodies have been shown to protect non-human primates against infection by passive transfer [22]. This provides hope that these gp41 and gp120 bnAbs, if elicited by vaccination, could provide protective immunity in humans.

### **Vaccine development**

HIV-1 envelope proteins, gp120 and gp41 are the major targets of HIV-1 vaccine development [4]. Epitopes that are targeted by bnAbs provide insight into the vulnerabilities of the viral envelope [23]. Immunogens that correctly represent the structure and context of these viral epitopes will, upon immunization, have the greatest chance of eliciting neutralizing antibodies *in vivo* [24]. Many HIV-1 vaccines have been developed since the discovery of HIV-1 over 30 years ago. However, none have been successful in eliciting sterilizing protection against HIV-1 infection.

Initial HIV-1 vaccines consisted of synthetic peptides or monomeric, recombinant envelope proteins (rgp120 or rgp160) produced in baculovirus, yeast or mammalian cells [25]. Most vaccine products were subtype B and had little genetic variability. HIV-1 specific antibodies were elicited but were strain-specific and were not capable of neutralizing diverse virus strains [25]. Contemporary vaccines reflect a larger genetic

diversity of HIV-1 and involve more complex strategies, including live vector vaccines, whole-inactivated vaccines, and trimeric envelope proteins [6,26]. Antibodies that are elicited during vaccination with these products are capable of neutralizing some strains of HIV-1 *in vitro* and have been shown to be moderately effective *in vivo*. These vaccines have improved humoral and cellular responses but have not achieved the ultimate goal of protective immunity [27].

Vaccines engineered to induce neutralizing antibodies face several challenges. HIV-1 subtypes are genetically distinct and have extensive sequence variation within each subtype; antibodies directed against one subtype or strain may not be cross-reactive against another [14,28]. Conserved regions of gp120 and gp41 exist but are camouflaged by variable loops, occluded by the trimeric envelope structure or quickly masked by mutation in surrounding regions [18]. HIV-1 has an error-prone reverse transcriptase resulting in changes in envelope structure and glycosylation patterns that rapidly leads to immune evasion [29]. An effective vaccine must overcome these obstacles.

HIV-1 vaccine design requires more in-depth understanding of epitope context and structure. A high-resolution crystal structure of the gp120/gp41 envelope trimer does not exist. Fragments of gp41 have been characterized but the hydrophobic nature of the protein hinders full-length protein production and purification. The structure and function of gp41, a transmembrane protein, are affected by the lipid composition of the surrounding membrane [30]. Gp120 and gp41 are highly dynamic proteins that undergo significant transitions during the infection process; understanding the structure of the native and transitions states will facilitate vaccine design [21,31].

An effective HIV-1 vaccine will elicit antibodies that are capable of binding to the envelope glycoprotein and inhibiting HIV-1 infection *in vivo*. Viral epitopes contained in the vaccine must be present and exposed on the surface of HIV in order for the elicited antibody to neutralize HIV-1 [32]. Antibodies that bind to HIV-1 in the native state may have greater opportunity to neutralize the virus than those that bind to HIV-1 in the receptor-bound state, as viral fusion can occur in as little as 10 minutes after CD4 binding [33]. Therefore it's important to understand the exposure and accessibility of vaccine-targeted HIV-1 epitopes.

### **MPER as a target for HIV-1 vaccine design**

The MPER of gp41 is a novel target for HIV-1 vaccine development. This region is critical for HIV-1 infection and is therefore highly conserved among diverse strains of HIV-1 [19]. Gp41 has less sequence variability than gp120 and contains fewer glycosylation sites, it is therefore less likely to be protected by mutation and glycan shielding [34]. The MPER is a linear stretch of 23 amino acids, containing epitopes for three known bnAbs, 4E10, 2F5 and Z13 (Figure 4). 4E10 is one of the most broadly neutralizing HIV-1 antibodies known and is effective against viruses from every subtype [35].

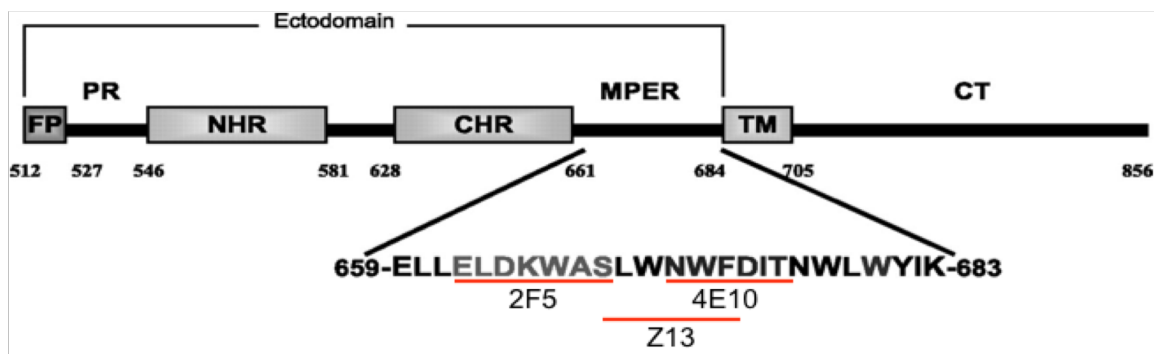


Figure 4. Diagram of gp41 indicating the amino acid location, sequence and bnAb epitopes within MPER [19].

MPER structure has not been fully characterized. It has been predicted to be both an  $\alpha$ -helical and an extended  $\beta$ -turn motif, assuming irregular structures that align in parallel with the adjacent membrane surface [36,37,38]. Variation in predicted structure may represent the different structural states in which MPER may exist, from native to post-fusion. This flexible region is further restructured upon antibody binding. It is thought that 4E10 extracts the MPER epitope from the lipid membrane, 2F5 lifts the N-terminal region and Z13 binds directly to the center region of the MPER epitope (Figure 5) [39,40]. These induced structural changes further confound our understanding of epitope structure required to elicit neutralizing antibodies.

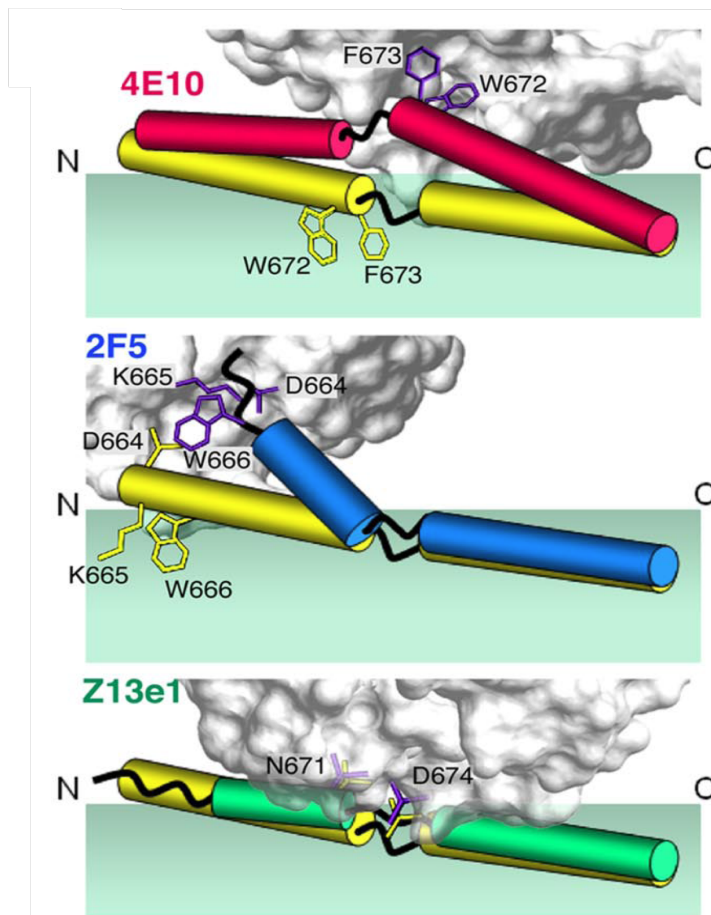


Figure 5. Representation of MPER orientation changes induced by 4E10, 2F5 and Z13 binding. Unbound peptide (yellow) is embedded in the viral lipid bilayer (green), antibody-complexed MPER conformational changes are shown in red, blue and green [39].

The HIV-1 membrane is important for MPER structure and function as well as antibody binding. 4E10, which binds to the most C-terminal region of MPER, adjacent to the transmembrane region, has been shown to interact with a variety of lipid components within the membrane (Figure 6) [41]. Antibody binding to viral lipids before binding to the MPER region of gp41, may increase the overall affinity of the antibody for the MPER epitope [42]. Mutational studies have shown that the neutralization potency of

4E10 is not dependent on lipid binding [43]. However, incorporation of lipid in immunogen design may facilitate production of these cross-reactive antibodies.

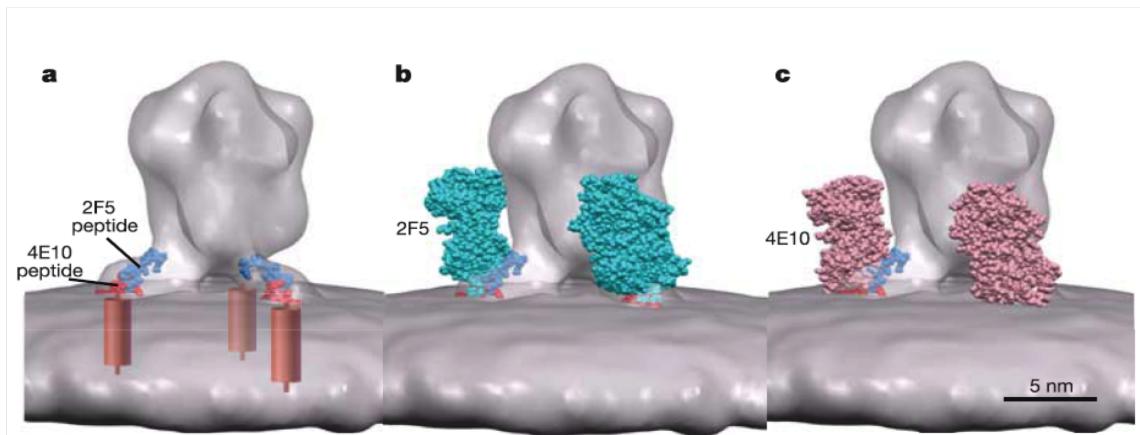


Figure 6. Surface-rendered model of the envelope spike showing a) positioning of 2F5 and 4E10 epitope and the proposed position of antibody-binding fragment (Fab) of 2F5 (blue, b) and 4E10 (red, c) [44].

While the MPER is the major target of 4E10, this antibody has also been shown to interact with the N-terminal region of gp120, the N-terminal gp41 fusion peptide, and the gp41 cytoplasmic tail [11,45,46]. 4E10 may also interact with unknown viral or cellular components. The antibody-combining site, the portion of the antibody that physically contacts the antigen, of 4E10 is considerably longer and more hydrophobic than most antibodies [47]. Only two residues at the base of the complementarily-determining region (CDR) of the third heavy chain (H3) have been shown to contact the MPER epitope; the apex of the loop orients away from this region and is thought to have uncharacterized binding partners [48]. CDR-H3 lies at the center of the antigen-combining site and is critical for antigen recognition. Understanding the full epitope of this broadly neutralizing antibody is required for MPER-directed vaccine design.

The lack of critical information in the MPER region is evident in the failure of MPER-specific vaccines to induce bnAbs. Attempted vaccines have included MPER peptides [49,50,51,52], truncated gp41 proteins [53,54], full-length gp145 proteins [55,56,57], and epitope scaffolds [58,59,60]. Immunogens have included peptides or proteins, either alone or in combination with lipid components [61]. These designs have been unsuccessful in part due to the hydrophobic nature of the MPER and gp41 in general. Gp41 is difficult to produce, usually requiring significant mutation or truncation to produce in sufficient quantities for preclinical vaccine testing. Protein modifications may interfere with the native conformational arrangement of the MPER epitope, presenting it in an immunologically irrelevant way.

#### **Development of the humoral immune response to HIV-1 MPER.**

Neutralizing antibodies, while difficult to elicit by vaccination are produced over the course of HIV-1 infection. The majority of these antibodies have limited breadth and potency; they are effective only against the infecting strain of HIV-1 [62]. Early antibodies target epitopes on gp120 and gp41 that can mutate to escape neutralization, limiting their effectiveness [63]. Approximately 10-30% of HIV-1 infected individuals develop a broad, cross-reactive neutralizing antibody response within the first 2.5 years of infection [64,65].

Antibodies directed against the MPER have been detected in roughly a third of HIV-1 infected individuals, however 2F5 and 4E10-like antibodies are thought to be rare [66]. MPER-specific antibodies have been shown to contribute to the overall neutralization breadth of HIV-positive plasma and in some rare cases may be responsible



for greater than 50% of the activity [67]. Plasma antibodies to MPER have unique specificities, as shown by alanine scanning, that need to be further characterized [68]. MPER can be recognized in a variety of conformations by the immune system, understanding the unique immunogenic structures of the MPER may identify novel targets for vaccine design.

### **Purpose of research**

We hypothesize that HIV-1 epitopes that are recognized with high affinity by known bnAbs will improve immunogen design and induce bnAbs. This is particularly critical for 4E10 where MPER structure is poorly defined and potentially unknown binding partners exist. This study has four specific aims that are designed to test this hypothesis: **1)** To characterize the neutralization profile of MPER-specific bnAbs and plasma antibodies and to explore the accessibility of viral MPER; **2)** To reconstruct the MPER bnAb epitopes using random-peptide library biopanning strategies, identifying novel epitopes that may provide insight into the structure of the native and transition states of MPER; **3)** To identify neutralization-competent MPER structures by characterizing the HIV-positive *in vivo* response to high-affinity MPER epitope variants and determining the neutralization efficacy of epitope-specific antibody populations; and **4)** To test the immunogenicity of neutralization-competent MPER variants, alone and in combination, with an established immunogen.

### **Overview of experimental designs**

**1. MPER-directed neutralization:** Neutralization breadth and potency of MPER bnAbs, 2F5 and 4E10, were assessed *in vitro* against a multi-subtype panel of HIV-1

isolates. HIV-1 envelope sequences were compared to identify resistance-causing mutations. Virus capture assays were performed to assess accessibility of the MPER epitope in native and receptor-bound HIV-1 states. HIV-positive plasma samples were analyzed to determine frequency and potency of anti-MPER response *in vivo*.

**2. BnAbs epitope reconstruction:** Biopanning of random peptide libraries was used to select high-affinity epitope variants that bind to MPER bnAbs. Two phage display random peptide libraries were used, Ph.D.12 and Ph.D.c7c, expressing linear 12-mers or disulfide-constrained 7-mers fused to the minor coat protein g3p of M13 bacteriophage. Several biopanning strategies using an antibody-coated surface were attempted. The peptide library was: i) bound directly to the antibody under stringent conditions, ii) bound in competition with HIV-1, with or without soluble CD4, or iii) bound in the presence of antibody:HIV-1 complex. Variants of the known linear epitopes as well as novel, structural epitopes were identified. Relative affinity and specificity of the selected epitopes were determined by M13 binding ELISA and peptide competition assays. Virus capture competition assays determined if the M13-displayed epitopes could compete with HIV-1 for antibody binding. Selected peptide epitopes were modeled to predict the structure of the epitope recognized by the bnAbs.

**3. MPER humoral recognition *in vivo*:** The antibody response to MPER during HIV-1 infection was characterized using the bnAb-selected, M13-displayed epitopes. HIV-positive plasma IgG bound to protein A-coated magnetic beads were used to immunoprecipitate select, high-affinity M13-displayed MPER epitopes variants. Immunoblot detection of the M13 major coat protein P8, approximately 2700 copies per

phage, greatly amplified the signal from antibodies present in minute amounts in typical patient plasma. Recognition by HIV-positive patient antibody would suggest that the epitope in question was displayed on HIV-1 and was able to induce an antibody response during the course of infection. M13-displayed epitopes were used to absorb epitope-specific plasma antibodies; the decrease in neutralization capacity was tested.

**4. Immunogen development:** Immunogenicity of select M13-displayed 4E10 epitopes, those capable of mitigating antibody-mediated neutralization, were tested by vaccination of mice. MPER variants were used alone, in combination with other MPER variants, or in combination with an HIV-1 envelope antigen. The elicited immune responses were analyzed for HIV-1 envelope binding and anti-HIV-1 humoral and cellular immune responses.

### **Originality and contribution**

This study will generate insights into the challenging problem of HIV-1 vaccine design. Specifically, the proposed research will identify novel epitopes recognized by MPER bnAbs and distinguish unique binding profiles to these epitopes by HIV-positive plasma antibodies. The neutralization potency of epitope-specific antibody populations will provide information on the nature of the target epitopes that can elicit a broadly protective immune response. Using these epitopes to boost epitope-specific immune responses could lead to the development of an efficacious HIV-1 vaccine.

## **Material and Methods**

### **Section 1. MPER-directed neutralization**

#### **TZMbl cells**

TZM-bl is a CXCR4<sup>+</sup> HeLa cell clone that was engineered to express CD4 and CCR5 receptors. The cells contain an integrated, firefly luciferase reporter genes under control of an HIV-1 long-terminal repeat sequence. Expression of the reporter gene is induced in trans by HIV-1 Tat protein shortly after infection. Luciferase activity is measured by luminescence and is directly proportional to the number of infectious virus particles present in the initial inoculum [69].

#### **HIV-1 Isolates**

Full-length, gp160 envelopes were cloned from 56 of 60 strains from a well-characterized panel of HIV-1 primary isolates (10 from each major clade; A, B, C, D, CRF01\_AE and CRF02\_AG), and used to generate pseudovirus stocks (Table 1) [70].

Subtype	Isolate Name	Origin	Correceptor Use
A	92/UG/029	Uganda	CXCR4
A	93/RW/024	Rwanda	CXCR4/CCR5
A	KER 2008	Kenya	CXCR4/CCR5
A	KER 2018	Kenya	CCR5
A	KNH 1088	Kenya	CCR5
A	KNH 1135	Kenya	CCR5
A	KNH 1144	Kenya	CCR5
A	KNH 1209	Kenya	CCR5
A	KSM 4030	Kenya	CCR5
B	33931N	United States	CCR5
B	873	United States	CCR5
B	BAL	United States	CCR5
B	BK 132	Thailand	CXCR4
B	BXO 8	France	CCR5
B	BZ 167	Brazil	CXCR4
B	MN-P	United States	CXCR4
B	NP 1538	Thailand	CCR5
B	US 1	United States	CCR5
B	US 4	United States	CCR5
C	20635-4	India	CCR5
C	56313	United States	CCR5
C	93/MW/965	Malawi	CCR5
C	GS-015	Senegal	CCR5
C	GS-016	Senegal	CCR5
C	PBL 286(696)	Ethiopia	CCR5
C	TZA 125	Tanzania	CCR5
C	TZA 246	Tanzania	CCR5
C	PBL 288(411)	Ethiopia	CCR5
C	TZBD 9/11	Tanzania	CCR5
D	57128	Uganda	CCR5
D	93/UG/065	Uganda	CXCR4
D	A03349M1	Uganda	CCR5
D	A07412M1	Uganda	CCR5
D	A08483M1	Uganda	CCR5
D	D26830M4	Uganda	CCR5
D	E08364M4	Uganda	CCR5
D	E13613M4	Uganda	CCR5
D	NKU 3006	Kenya	CCR5
CRF02_AG	55815	United States	CCR5
CRF02_AG	CAM 0002 BBY	Cameroon	CCR5
CRF02_AG	CAM 0005 BBY	Cameroon	CCR5
CRF02_AG	CAM 0008 BBY	Cameroon	CCR5
CRF02_AG	CAM 0013 BBY	Cameroon	CCR5
CRF02_AG	CAM 0014 BBY	Cameroon	CCR5
CRF02_AG	CAM 0015 BBY	Cameroon	CCR5
CRF02_AG	CAM 1475 MV	Cameroon	CCR5
CRF02_AG	CAM 1970 LE	Cameroon	CCR5
CRF02_AG	DJ 263	Djibouti	CCR5
CRF01_AE	CM 235	Thailand	CCR5
CRF01_AE	CM 240	Thailand	CCR5
CRF01_AE	CM 244	Thailand	CCR5
CRF01_AE	0503M02138	Thailand	CXCR4
CRF01_AE	NI 1052	Thailand	CXCR4
CRF01_AE	NI1149	Thailand	CCR5
CRF01_AE	NI1046	Thailand	CCR5
CRF01_AE	NP1695	Thailand	CXCR4

Table 1: Multi-subtype panel of HIV-1 isolates.

HIV-2 chimeric envelope containing the HIV-1 MPER and HIV-2 envelope without MPER were used to generate pseudoviruses that specifically measure MPER-specific neutralization and non-specific inhibition.

Pseudoviruses containing either the envelope glycoprotein from murine leukemia virus (MuLV), vesicular stomatitis virus (VSV) or no envelope glycoprotein (Bald) were used as negative controls to measure non-specific viral inhibition.

### **Pseudovirus preparation**

Pseudoviruses were produced in 293T cells by co-transfection of two plasmids; an Env expression plasmid containing the viral envelope of choice and an HIV-1 backbone plasmid (pSG3ΔEnv) containing the entire HIV genome with the exception of Env. The pSG3ΔEnv plasmid is transcribed into viral genomic RNA and packaged by the pseudovirus; the Env plasmid is not packaged. The resulting pseudovirus particles are therefore limited to one round of infection. Pseudoviruses were prepared by transfecting  $5 \times 10^6$  293T cells with 8 µg of *env* expression plasmid and 24 µg of pSG3ΔEnv, using FuGene transfection reagent (Roche Diagnostics). Cultures were incubated at 37°C in a humidified 5% CO<sub>2</sub> incubator for 72 h, supernatants were centrifuged, filtered and stored at – 80°C until use.

### **Pseudovirus neutralization assay**

TZM-bl cells were used as assay targets to determine HIV-1 neutralization. BnAb or plasma were titrated in 4-fold serial dilutions starting at 25 µg/ml or 1:20 dilution respectively, in growth medium [DMEM with 100 U/ml penicillin, 100 µg/ml streptomycin, 2 mM L-glutamine (Quality Biologics Inc.), and 15% fetal calf serum

(Gemini Bio-Products)] and 25  $\mu$ l added in duplicate to a 96-well flat-bottom black plate. Pseudovirus, diluted in growth medium to a dilution optimized to yield ~150,000 relative luminescence units (RLU), was added in equal volume to each well. The samples were incubated at 37°C in a humidified 5% CO<sub>2</sub> incubator for 1 h. All incubations were under these conditions. TZMbl cells were resuspended at  $2 \times 10^5$  cells/ml in growth medium containing 60  $\mu$ g/ml DEAE-dextran (Sigma), 50  $\mu$ l was added to each well. Each plate included wells with cells and pseudovirus (virus control) or cells alone (background control). Plates were incubated for 48 h, and then 100  $\mu$ l/well of reconstituted Brite Lite Plus (Perkin Elmer) was added. RLU values were measured using a Victor 2 luminometer (Perkin-Elmer). The percent inhibition due to the presence of the antibody was calculated by comparing RLU values from wells containing antibody to well with virus control. Two independent assays were performed and the results were averaged [69,71].

### **HIV-1 capture assay**

4E10 and 2F5 binding to HIV-displayed epitopes was quantified using HIV-1 capture assays. 4E10- and 2F5-neutralization sensitive isolates from subtype A (KSM4030 and KER2008) and subtype B (873 and BK132) and 4E10- and 2F5-neutralization resistant isolates from subtype A (92/MG/024 and KER2018) and subtype B (US1 and 33931) were analyzed. Reacti-Bind Protein A/G Coated 96-well plates (Pierce) were wash three times with 300  $\mu$ l 0.05% PBST (PBS containing 0.05% Tween-20). Antibodies were diluted to 10  $\mu$ g/ml in SuperBlock Blocking Buffer (Pierce), 100  $\mu$ l/well were added to the plate. Plates were incubated at room temperature for 1 h with gentle agitation then washed three times with 300  $\mu$ l 0.05% PBST (PBS containing

0.05% Tween-20). Plates were blocked with 300  $\mu$ l SuperBlock Blocking Buffer for 1 h with gentle agitation then washed three times with 300ul 0.05% PBST. HIV-1 pseudovirus stocks were titrated 3-fold in RPMI-1640 starting at 17.5 ng/ml p24. 100  $\mu$ l of each dilution was added to the plate in duplicate. Plates were incubated at 37°C for 1 h then washed six times with 300  $\mu$ l RPMI-1640. Disruption buffer was added to each well and bound pseudoviruses were quantitated by p24 ELISA. Assays measuring the effect of sCD4 binding on HIV-1 capture were performed using HIV-1 stocks that were pre-incubated with 10  $\mu$ g/ml sCD4 at 37°C for 1h before titration and addition. All assay manipulations involving HIV-1 were performed in a biological safety cabinet. Two independent assays were performed and the results were averaged.

#### **p24 ELISA**

Pseudovirus particle number was estimated by determination of p24 capsid protein concentration of the viral stock. ELISAs were performed using HIV-1 p24 Antigen Capture Assay (Advanced BioScience Laboratories, Inc) with some modifications to the manufactures protocol. Samples were lysed by adding disruption buffer (PBS containing 2.5% Triton-X), diluted in PBS containing 0.05% BSA, then 100  $\mu$ l was added to the ELISA microplate containing a protein standard. The plates were incubated at 37°C for 1 h then washed six times with wash buffer (PBS containing Tween-20). Horseradish peroxidase-labeled conjugate was added, plates were incubated at 37°C for 1 h then were washed six times with wash buffer. Peroxidase substrate was added; plates were incubated at room temperature for 15 min, then the reaction was stopped by adding Stop solution (2N sulfuric acid). Plates were read on a



spectrophotometer at 450 nm and the protein concentration determined based on the standard curve.

## **Section 2. bnAb epitope reconstruction**

### **Phage display libraries**

Two phage display random peptide libraries, Ph.D.12 and Ph.D.c7c (New England Biolabs), were used to select high-affinity epitope variants that bound to MPER bnAbs. The libraries express linear dodecapeptides (Ph.D.12) or disulfide-constrained heptapeptides (Ph.D.c7c) fused to the minor coat protein g3p of M13 bacteriophage. G3p-fused epitopes, displayed as five copies clustered at one end of the mature M13 virion, do not effect infectivity of the bacteriophage. M13 DNA has also been modified to include the lacZ $\alpha$  gene; plaques appear blue when plated on Xgal containing agar. Each library has a complexity on the order of  $10^9$  independent clones [72].

### **E. Coli Strain**

E. coli host strain ER2738 ( $F'$  proA<sup>+</sup>B<sup>+</sup> lacI<sup>q</sup>  $\Delta$ (lacZ) M15 zzf::Tn10 (Tet<sup>R</sup>)/fhuA2 glnV  $\Delta$ (lac-proAB)  $\Delta$ (hsdMS-mcrB)5 [ $r_k^- m_k^-$  McrBC<sup>-</sup>]) was used for M13 propagation. ER2738 is a robust F<sup>+</sup> strain with a rapid growth rate and is well-suited for M13 propagation. The F-factor of ER2738 contains a mini-transposon, which confers tetracycline resistance. E. coli stocks, produced from single colonies grown on LB/Tetracycline plates, were cultured overnight in LB/Tetracycline liquid medium [72].

### **BnAb epitope selection by biopanning**

Biopanning experiments were performed in 96-well microtiter Immunol B polystyrene plates (Figure 7). Antibody (4E10, 2F5 or Z13) was diluted to 6.7  $\mu$ g/ml in

0.1 M NaHCO<sub>3</sub>, 150 µl was added to each target well. The plate was incubated overnight at 4°C with gentle agitation in a humidified container. The unbound target antibody was removed and the plate blocked with 300 µl of 10% nonfat milk at 4°C for 1 h. The plate was washed six times with 300 µl of 0.1% PBST (PBS containing 0.1% Tween-20). M13 library was added,  $1 \times 10^{11}$  M13/well in 0.1% PBST, and incubated at room temperature with gentle rocking for 5 min. Unbound M13 were removed by washing the plate ten times with 300 µl 0.1% PBST. Bound M13 were eluted with 100 µl of 0.2 M Glycine-HCl (pH 2.2); elution buffer was incubated for 10 min at room temperature with gentle rocking. Eluted phage were transferred to a microcentrifuge tube where the pH was neutralized by adding 15 µl of 1 M Tris-HCl (pH 9.1). Eluted phage were titered on LB/IPTG/Xgal plates and amplified on E. coli. Amplified M13 cultures were used as input for two additional rounds of biopanning.

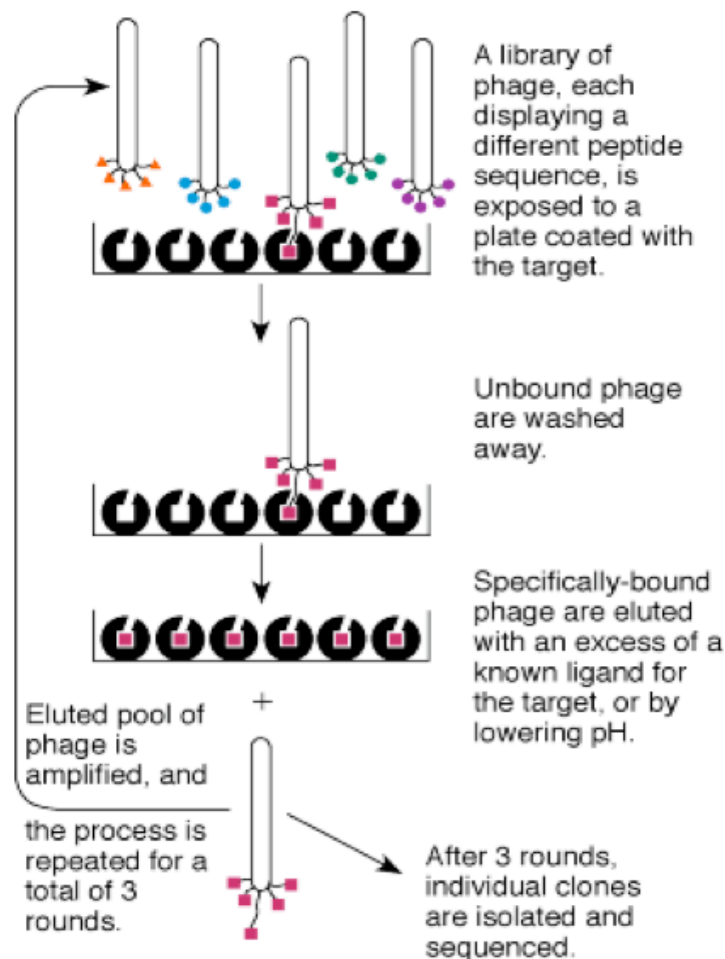


Figure 7. Diagram of phage display biopanning procedure.

Several selection strategies were attempted in additional rounds. 1) The stringency of selection was increased by using wash buffer with increased tween-20 concentration, 0.5% PBST. 2) The target antibody was bound to HIV-1 pseudovirus before the addition of the M13 library. HIV-1 pseudovirus, clade B 873, was added at a concentration of 17.5 ng/ml p24, 30 min before the direct addition of M13. 3) HIV was also pre-incubated with sCD4 for 30 min at 20  $\mu$ g/ml before adding to the target plate.

Experiments using HIV-1 were performed in a biological safety cabinet; HIV-1 was inactivated with disruption buffer after elution [72].

### **M13 amplification and purification**

M13 clones were amplified by infection of 20 ml mid-log culture of ER2738 by a single plaque or  $10^{10}$  phage particles. Cultures were incubated at 37°C with rapid rotation for 5 h. Supernatants were transferred to 30 ml tubes and centrifuged at 4500 g for 10 min at 4°C, twice. M13 were precipitated by adding 1/6 volume of 2.5 M NaCL/20% PEG-8000 for 1 h at 4°C. Samples were centrifuged at 12000 g for 15 min at 4°C. Supernatant was decanted, the pellet was resuspended in 1 ml PBS then transferred to an eppendorf tube and briefly centrifuged to remove any remaining bacteria. Supernatants were transferred to fresh eppendorf tubes, 1/6 volume of 2.5 M NaCL/20% PEG-8000 was added then samples were incubated on ice for 30 min. Samples were centrifuged at 16000 g for 10 min at 4°C. Supernatants were removed, the tubes were briefly centrifuged and remaining supernatants were removed. Phage pellets were resuspended in 200 µl PBS and the phage concentration was determined by spectrophotometry and infectious titer. Samples were aliquoted and stored at -20°C [72].

### **M13 DNA purification and sequencing**

M13 DNA samples were prepared for sequencing using QIAprep Spin M13 Kit (Qiagen), following the manufactures protocol [73]. All centrifugation of QIAprep spin columns were carried out in a conventional tabletop microcentrifuge at 8000 rpm. Culture supernatants collected after two rounds of centrifugation, 1 ml of cleared culture was used for DNA purification. M13 were precipitated by adding 10 µl M13 precipitation

buffer, samples were vortexed and incubated at room temperature for 2 min.

Supernatants were transferred to a spin column in a microcentrifuge tube and centrifuged for 15 s. Bacteriophage were retained on the silica –gel column membrane, flow-through was discarded. A high-salt M13 lysis buffer was added (0.7 ml), the column was incubated at room temperature for 1 min, centrifuged for 15 s then the flow-through was discarded, twice. Phage particles were lysed and removed while the single-stranded DNA was absorbed onto the membrane. The column washed once by adding 0.7 ml wash buffer, centrifuging for 15 s and discarding flow-through. The column was then centrifuged for an additional 15 s to dry the membrane, removing residual wash buffer. The column was placed into a fresh microcentrifuge tube, 100 µl of elution buffer (10nM Tris-Cl, pH 8.5) was added then incubated for 10 min and centrifuged for 30 s at 8000 rpm. Flow-through was collected and DNA was sequenced by either Davis Sequencing (Davis, CA) or Retrogen Inc. (San Diego, CA). Sequencing primer 96 gIII (NEB #S1259S) was used.

### **Sequence alignment**

Insert sequences were aligned using ClustalW Multiple Sequence Alignment. Insert sequences and alternative 4E10-HIV-1 epitope sequences were aligned using Pairwise Sequence Alignment. Both programs are available at [www.ebi.ac.uk/](http://www.ebi.ac.uk/)

### **M13 binding ELISA**

The affinity and specificity of M13-displayed epitopes were determined by binding ELISA titration using specific (4E10, 2F5 or Z13) and nonspecific (2G12) target antibodies. Antibodies were diluted to 10 µg/ml in 0.1 M NaHCO<sub>3</sub> (pH 8.6), 100 µl per

well was added to 96-well microtiter Immunol B polystyrene plates. Plates were incubated overnight at 4°C with gentle agitation in a humidified container then washed three times with 300 µl 0.05% PBST (PBS containing 0.05% Tween-20). Plates were blocked with 300 µl 10% non-fat Milk for 1 h at 4°C then washed twice with 0.05% PBST. M13 was titrated in 2-fold serial dilutions starting at  $1 \times 10^{11}$  M13/ml in 10% non-fat milk and 100 µl added to the plate. Plates were incubated at room temperature for 1 h then washed three times with 300 µl 0.05% PBST. HRP-labeled anti-M13 antibody (Pharmacia, 27-9411-01) diluted to 1:5000 in 10% non-fat milk was added, 100 µl/well. Plates were incubated for 30 min at room temperature then washed three times with 300 µl 0.05% PBST. TMB (KPL, 50-76-03) (100 µl) was added, incubated for 15 min at 37°C and the reaction stopped by adding 100 µl of 1M phosphoric acid. Plates were read on a spectrophotometer at 450 nm. M13 binding titer was determined by calculating the M13 concentration at which binding was detectable above five times background, M13 binding to uncoated wells. Two independent assays were performed and the results were averaged.

### **Peptide competition ELISA**

The M13 Binding ELISA was modified to include peptide competition. Tested peptides:

MPER peptide	LELDKWASLWNWFNITNWLWYIK(amide)
gp41 fusion peptide	GAVFLGFLGAAGSTM
gp41 endodomain	AVAEGTDRIIELIQR
gp120 N-terminus	LWVTVYYGVPVWKEA, VYYGVPVWKEAKTTL

MPER scrambled peptide      LSINEAFKWLDWWTLNDLWYIWK(amide)

Nonspecific peptide          DRLGRIIEEGGEQDR

Lyophilized peptides were reconstituted in methanol at 2 mg/ml and were stored at -20°C. Assay plates were coated with specific antibody and blocked as described above. A single concentration of M13 ( $7.5 \times 10^8$  M13/ml) and titrated peptide (5-fold serial dilutions starting at 100 µg/ml) were added concurrently to each well. Samples were incubated at room temperature for 1 h, the rest of the assay proceeded as described for the M13 Binding ELISA. Peptide inhibition was determined by comparing wells containing peptide to wells without peptide. Two independent assays were performed and the results were averaged.

#### **HIV-1 capture competition assay**

The HIV-1 capture assay was modified to include M13-displayed epitope competition in which HIV-1 and M13 were added to the plate together. M13 was titrated in 2-fold serial dilutions starting at  $4 \times 10^{11}$  M13/ml in RPMI-1640; HIV-1 pseudoviruses were diluted in RPMI-1640 to 35 ng/ml p24. Equal volumes of M13 and HIV were added concurrently to each well. All other steps were performed as described for the HIV-1 capture assay.

#### **Structural modeling**

The N-terminal region of the M13 g3p protein containing the bnAb-selected epitopes were modeled using HHpred (homology detection and structure prediction by pairwise comparison of profile hidden Markov models) and secondary structure was

predicted using Jpred3 (structure prediction by neural network assignment). Molecular visualization and editing was performed using Pymol.

### **Section 3. MPER humoral recognition *in vivo***

#### **Immunoprecipitation**

HIV-positive plasma IgG was bound to magnetic protein A-coated beads then used to immunoprecipitate M13-displayed MPER epitopes. Protein A beads (Invitrogen) were resuspended and 50  $\mu$ l per samples was transferred to an eppendorff tube. Tubes were placed in a magnetic rack and residual liquid was removed. The beads were washed by resuspending in 200  $\mu$ l PBST 0.05% then liquid was removed after 1 min on a magnetic rack. The beads were resuspended in 200  $\mu$ l antibody binding buffer (PBST 0.02%) containing 1.5  $\mu$ l of filtered undiluted plasma. This concentration of plasma IgG will saturate the protein A beads. The protein A beads and plasma IgG were mixed by rotation at room temperature for 30 min. The tubes were then placed in a magnetic rack and liquid was removed. The beads were then washed three times with 200  $\mu$ l PBST 0.05%, the samples were transferred to new eppendorff tubes twice between washes. The beads were resuspended in 200  $\mu$ l 10% nonfat milk and were mixed by rotation at room temperature for 30 min. Tubes were placed on the magnetic rack and liquid was removed after 1 min. The beads were resuspended in 200  $\mu$ l 10% nonfat milk containing  $1 \times 10^{10}$  M13/ml and were mixed by rotation at room temperature for 30 min. The beads were then washed seven times with 200  $\mu$ l PBST 1.5%, the samples were transferred to new eppendorff tubes three times between washes. The beads were resuspended in 20  $\mu$ l elution buffer (0.2 M Glycine-HCl, pH2.2) and incubated at room temperature for 5 min.



The tubes were placed on a magnetic rack for 1 min, the eluate was removed into a fresh eppendorff tube then M13 capsid protein was detected by western blot.

### **Western Blot**

Samples were prepared by mixing 20 µl sample with 20 µl 2x SDS and 4 µl 10x reducing reagent. Sample were boiled for 5 min then mixed by brief centrifugation. Novex 16% gels (Invitrogen) were loaded with 8 µl sample per well. Gels were run for 1.5 h at 125 V with Novex running buffer (Invitrogen). Separated proteins were transferred to a PVDF 0.2 µm membrane (Invitrogen) for 50 min at 25 V using Novex transfer buffer (Invitrogen). The membrane was then rinsed twice with 10 mls water for 5 min. All incubations were performed at room temperature on a plate tilter set to one rotation per second. The membrane was blocked with blocking buffer (Li-Cor Biosciences) for 30 min then rinsed twice with 10 mls water for 5 min. Murine primary M13 g8p antibody (AbCam) was diluted 1:1000 in 10 mls blocking buffer and incubated with the membrane for 60 min. The membrane was washed four times with wash buffer (TBST 0.05%). Secondary IRdye conjugated goat anti-mouse IgG antibody (Li-Core) was diluted 1:10,000 in 10 mls blocking buffer and incubated with the membrane for 45 min. The membrane was washed four times with wash buffer then rinsed twice with 10 mls water. The membrane was dried and scanned using an Odyssey infrared imaging system (Li-Core). Bands were normalized and quantified using protein standards.

### **Pseudovirus neutralization competition assay**

The pseudovirus neutralization assay protocol was used with the following modifications. The MPER-chimera pseudovirus was used to assess neutralization

competition in this assay. Plasma was diluted to a final dilution of 2xID<sub>50</sub> and mixed with equal volume of M13 at a final concentration of  $5 \times 10^{10}$  M13/ml. The samples were incubated for 30 min. Pseudovirus was added in equal volume to each well, samples were incubated for an additional 30 min. TZMbl cells were resuspended at  $2 \times 10^5$  cells/ml in growth medium containing 60 µg/ml DEAE-dextran, 50 µl was added to each well. Each plate included wells with cells, plasma and pseudovirus (plasma control), cells and pseudovirus (virus control) or cells alone (background control). Plates were incubated for 48 h then analyzed. All values were normalized to the plasma control, which equals 100 relative light units. Neutralization competition was determined by comparing RLU values from wells containing M13 to the plasma and virus controls. Two independent assays were performed and the results were averaged.

#### **Section 4. Immunogen development**

##### **Antigens**

The gp145 protein was produced from an envelope sequence isolated from an acute, subtype C infected individual from Tanzanian. The entire ecto-domain of the protein is present, including the MPER of gp41. The protein was designed to include two mutations (R508S, R511S) in the gp120/gp41 cleavage site to prevent protease cleavage and a multi-lysine C-terminal to facilitate production and MPER epitope presentation. The protein was produced in CHO cells, purified by lectin affinity chromatography and is present as higher-order multimers. The gp145 protein contained the following MPER epitope sequence: ALDSWNNLWNWFDIS.

Five M13-displayed 4E10 epitopes, listed below, were produced in large volumes, PEG purified and resuspended in PBS as described above.

4E10 c7c4: cYFFDRSSc

4E10 12B6: DMRSIFHDNPFN

4E10 12B7: GYWSDYWGMTTH

4E10 12D1: QSYNWFDHTRWI

4E10 12D4: LPNWFNLSSNLM

### **Liposome preparation**

Antigens, M13 phage and gp145 protein, were encapsulated in liposome prior to immunization. Liposomes composed of dimyristoyl phosphatidylcholine, dimyristoyl phosphatidylglycerol and cholesterol in molar ratios of 1.8:0.2:1.5 were prepared by dispersion of lyophilized mixtures of lipids at a phospholipid concentration of 50 mM in Dulbecco's PBS with 0.4 g/ml lipid A, either lacking or containing antigen. Liposomes were washed twice in sterile saline to remove the unencapsulated antigen.

### **Animal Immunizations**

Forty female BALB/C mice, 25 g each, were immunized under a protocol approved by the Institutional Laboratory Animal Care and Use Committee. Animals were divided into eight groups of five animals each (Table 2). Mice were immunized intramuscularly four times in alternating caudal thigh muscles at two or three week intervals with  $5 \times 10^{11}$  phage or 10  $\mu$ g gp145 protein each per dose. Blood was collected at two-week intervals starting two weeks prior to the first immunization ending when the animals were euthanized. Blood was incubated at room temperature for 2-3 h,

refrigerated overnight at 4°C then centrifuged. Serum was collected and stored at -20°C. Two weeks after the last boost (week 10) the mice will be euthanized. Blood, spleens, lymph nodes, bone marrows, and livers were obtained and processed from naïve and immunized mice.

<b>Group#</b>	<b>Immunogen</b>	<b>Immunization (Weeks)</b>	<b>Bleeds (Weeks) 150ul/mouse/bleed</b>	<b>Euthanasia (collect blood, spleens, lymph nodes, bone marrow and livers)</b>
1	M13-12D4	0, 3, 6, 8	-2, 0, 2, 4, 6, 8, 10	Week 10
2	M13-12B7	0, 3, 6, 8	-2, 0, 2, 4, 6, 8, 10	Week 10
3	M13-all 5	0, 3, 6, 8	-2, 0, 2, 4, 6, 8, 10	Week 10
4	gp145/M13-all 5	0, 3, 6, 8	-2, 0, 2, 4, 6, 8, 10	Week 10
5	gp145	0, 3, 6, 8	-2, 0, 2, 4, 6, 8, 10	Week 10
6	M13-no insert	0, 3, 6, 8	-2, 0, 2, 4, 6, 8, 10	Week 10
7	Naïve	0, 3, 6, 8	-2, 0, 2, 4, 6, 8, 10	Week 10

Table 2. Mouse immunization plan.

### **IFN $\gamma$ -release ELISPOT (Enzyme-linked Immunosorbent Spot) assay**

Spleen cells secreting IFN $\gamma$  were analyzed by ELISPOT. Ninety-six-well nitrocellulose-backed MultiScreen-IP sterile plates (Millipore) were coated overnight at 4°C with 10  $\mu$ g/ml of anti-gamma interferon (IFN $\gamma$ ) (PBL Interferon Source) in sterile PBS. The wells were blocked with sterile PBS containing 0.5% bovine serum albumin for 30 min at 37°C and washed with PBS containing 0.025% Tween 20 (wash solution) followed by sterile RPMI-1640 complete medium. Single cell suspensions were prepared from the mouse spleens of each group (five mice/group). Cells ( $2 \times 10^6$ /well) were plated on anti-IFN $\gamma$ -coated plates and incubated for 18 h at 37°C in a humidified CO<sub>2</sub> incubator. Cells were incubated with 5  $\mu$ g/ml acute C gp145 (HIV-1 C06980, Advanced Bioscience Laboratories), gp140 (HIV-1 IIIB, Advanced Bioscience Laboratories), yeast-derived gp41 (Meridian Biosciences) or 10  $\mu$ g/ml cathepsin degraded, yeast-derived gp41 or no protein. Plates were washed with wash solution followed by distilled water and overlaid

with 0.125 µg/ml of biotinylated anti-IFN $\gamma$  (clone XMG 1.2; BD PharMingen) and incubated at room temperature for 2h. The plates were then washed and incubated with a 1:1,000 dilution of avidin-conjugated alkaline phosphatase (Vector Laboratories) for 2 h at room temperature. The plates were washed, and bound IFN $\gamma$  was detected by the addition of 5-bromo-4-chloro-3-indolylphosphate (BCIP)/nitroblue tetrazolium (NBT) (Kirkegaard and Perry Labs). The plates were washed with water, and the individual spots were visualized and counted the next day using a stereo binocular microscope. The average number of spots/number of cells plated was plotted.

#### **Antigen presentation and detection of cytokines from T-cells by flow cytometry**

Cells from spleens or lymph nodes from the different groups of mice were stimulated with 5 µg/ml acute C gp145 (HIV-1 C06980, Advanced Bioscience Laboratories), gp140 (HIV-1 IIIB, Advanced Bioscience Laboratories), yeast-derived gp41 (Meridian Biosciences) or 10 µg/ml cathepsin degraded, yeast-derived gp41 or ConA as the positive control for 22 h at 37°C. The cells were incubated with the above-mentioned antigens for 2 h before the addition of brefeldin A (1 mg/ml, Sigma-Aldrich) and monensin (0.07 mg/ml, BD Pharmingen). Cells were incubated for an additional 20 h. Cells were analyzed on a LSR II (BD Immunocytometry Systems) flow cytometer and 500,000 events were collected using FACSDiva software (BD Immunocytometry Systems). Dead cells were excluded using a viability marker and B-cells were excluded. The CD3<sup>+</sup> CD4<sup>+</sup> and the CD3<sup>+</sup> CD8<sup>+</sup> T-cells were gated and analyzed for the expression of, IL-2, TNF- $\alpha$ , IFN- $\gamma$  and CD107a. The data were analyzed using FlowJo software (Tree Star). Percent positively stained cells per antigen are shown for each

group. The black bar represents a two-fold range above the control response, M13 – no insert.

### **Antigen-specific serum IgG ELISA**

Antigen specific IgG titers were determined by binding ELISA titrations using gp145 and gp41 as targets. Antigens were diluted to 0.25 µg/ml in PBS (pH 7.4), 100 µl per well was added to 96-well microtiter Immunol 2 polystyrene plates. Plates were incubated overnight at 4°C then washed three times with 300 µl 0.1% PBST (PBS containing 0.1% Tween-20). Serum was titrated in 2-fold serial dilutions starting at 1:50 dilution in serum diluent (0.1% PBST containing 5% non-fat milk), and 100 µl each dilution was added to the plate. Plates were incubated at 37°C for 1 h then washed three times with wash buffer. HRP-labeled anti-mouse IgG antibody diluted to 1:16,000 in serum diluent was added, 100 µl/well. Plates were incubated for 1 h at 37°C then washed three times with wash buffer. TMB (100µl, Kirkegaard and Perry Labs) was added, incubated for 30 min at 37°C and the reaction stopped by adding 100 µl of 1 M phosphoric acid. Plates were read on a spectrophotometer at 410 nm, 570 nm reference filter. Antigen binding titer was determined by calculating the concentration at which binding was detectable above three times background. Two independent assays were performed and the results were averaged.

### **Surface Plasmon resonance (SPR) measurements by Biacore**

SPR measurements were conducted with a Biacore T200 using CM5 chips. Peptides were immobilized to the chip surface using the Biacore amine coupling kit (Biacore, AB). All immobilization steps used a flow rate of 10 µl/min and were

performed at 25°C. The peptide loading buffer was 20 mM sodium acetate, pH 4.2.

The immobilization wizard packaged within the T200 control software was used to immobilize 14700 resonance units (RU) of 10 uM scrambled MPER peptide and 20500 RU of MPER peptide to their respective flow cells. Both peptides had a 10 min contact time during immobilization. The serum samples were diluted 1:50 in Tris buffered saline, pH 7.4 and passed over the chip surface at 30 µl/min for 3 min followed by a 5 min dissociation period. At the end of the 5 min period, a 75 µg/mL solution of sheep anti-mouse IgG(Fc) antibody (The Binding Site) was passed over the flow cells for 2 min at a flow rate of 10 µl/min. After a 70 s dissociation period, the chip surface were regenerated using a 30 second pulse of 50 mM HCl, a 30 second pulse of 100 mM EDTA in 20 mM Tris, pH 7.4, and 30 second pulse of 50% acetic acid followed by a 1 minute injection of Tris-buffered saline, pH 7.4. Non specific binding was subtracted and data analysis was performed using the BIAevaluation 4.1 software. The reported response units for the IgG specific values are the difference between the average value of a 5 second window taken 60 seconds after the end of the anti-IgG injection and the average value of a 5 second window taken 10 seconds before the beginning of the anti-IgG injection.

### **Pseudovirus neutralization assay**

Neutralization assays were performed as described above.

### **PBMC neutralization assay**

PBMC, collected from HIV-negative donors and cryopreserved, were used as assay targets to determine HIV-1 neutralization. This assay uses replication-competent HIV-1 infectious molecular clones (IMC) containing a Renilla reniformis luciferase

(LucR)-expressing HIV-1 reporter gene; viral production is measured with a luminometer [74]. Sera were titrated in 4-fold serial dilutions starting at 1:20 dilution in IL-2 growth medium [RPMI-1600 with 100 U/ml penicillin, 100 µg/ml streptomycin, 2 mM L-glutamine (Quality Biologics Inc.), 15% fetal calf serum (Gemini Bio-Products), and 20 U/ml recombinant interleukin-2 (Roche Diagnostics)] and 25 µl was added in duplicate to a 96-well round-bottom plate. IMC, diluted in IL-2 growth medium to a dilution optimized to yield ~50,000 RLU, was added in equal volume to each well. The samples were incubated at 37°C in a humidified 5% CO<sub>2</sub> incubator for 1 h. All incubations were under these conditions. PHA/IL-2 stimulated PBMC were resuspended at  $2 \times 10^6$  cells/ml in IL-2 growth medium then 50 µl was added to each well. Each plate included wells with cells and IMC (virus control) or cells alone (background control). Plates were incubated for 24 h, 100 µl of growth medium was added to each well and then plates were incubated for an additional 72 h. Renilla Luciferase Assay System (Promega) was used to quantify luciferase production. Lysis buffer, 50 µl/well, was added and two freeze/thaw cycles were performed, 20 µl/well was transferred to a black, flat-bottom plate and RLU in each well were measured immediately after injection of 100 µl substrate. The percent inhibition due to the presence of the antibody was calculated by comparing RLU values from wells containing antibody to well with virus control. Two independent assays were performed and the results were averaged.



## **Results**

### **Section 1. Characterization of breadth and potency of MPER-directed antibodies**

The breadth and potency of 2F5 and 4E10 were assessed against a panel of 56 pure-subtype international HIV-1 isolates to determine their neutralization efficacy compared to two gp120 bnAbs. Epitope mutation and occlusion were explored as reasons for neutralization resistance. The effect of CD4-binding on MPER accessibility, for both neutralization sensitive and resistant isolates, was determined. Finally, a panel of twelve HIV-positive plasma samples was characterized to determine the neutralization potency of MPER-directed antibodies elicited during the course of infection. Epitope-specific neutralization was compared to overall neutralization capacity of the plasma sample.

#### **Characterization of 2F5 and 4E10 neutralizing activity**

A panel of 56 HIV-1 isolates was used to characterize the neutralization breadth and potency of 4E10 and 2F5. Isolates were chosen from six major HIV-1 subtype: nine from subtype A, 10 from subtype B, 10 from subtype C, nine from subtype D, eight from CRF01\_AE and 10 from CRF02\_AG (Table 1). Envelope genes were sequenced to confirm the isolates were selected from pure-subtype infections. The antibody concentration required to inhibit 50% of viral growth (IC<sub>50</sub>) was calculated, reported values are the mean of two independent, concordant assays (values are within 5-fold range). Two gp120 antibodies were used for comparison; 2G12 binds to mannose moieties and b12 binds to the CD4-binding site (Figure 8).

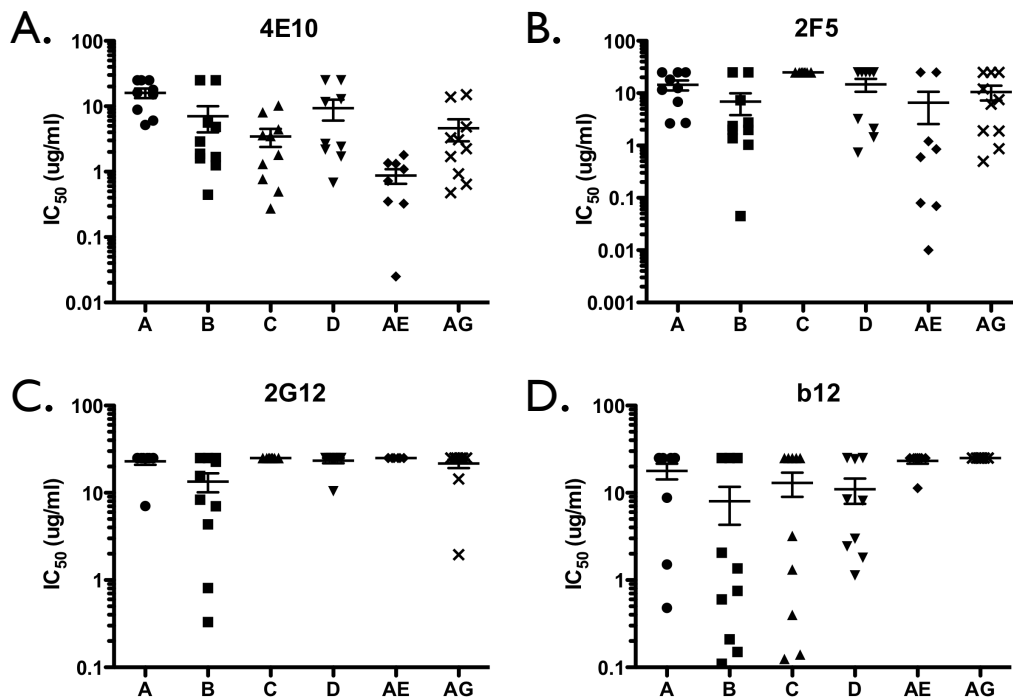


Figure 8. Neutralization profile of four bnAbs: a) 4E10, b) 2F5, c) 2G12 and d) b12 against HIV-1 isolates from subtype A, B, C, D, CRF01\_AE and CRF02\_AG.

4E10 and 2F5 are broadly and potently neutralizing antibodies. 4E10 neutralized 88% of the HIV-1 isolates tested, neutralizing viruses from every subtype with an average neutralizing titer of 4.3  $\mu$ g/ml. 2F5 neutralized 55% of all isolates tested, including isolates from all subtypes except subtype C; isolates from subtype C do not contain the 2F5 epitope due to mutation. The average neutralizing titer for 2F5 was 3.7  $\mu$ g/ml. b12 and 2G12 were found to be less broad, neutralizing 41% and 20% of isolates respectively.

In this panel of viruses, excluding the subtype C isolates which do not contain the 2F5 epitope, the neutralization profiles of 2F5 and 4E10 were linked. Of the 46 non-subtype C isolates, 36 had 2F5 and 4E10 IC<sub>50</sub> values (29 neutralization-sensitive (+)

isolates and 7 neutralization-resistant (-) isolates) that were within a five-fold range, the acceptance criteria for concordance within this assay. Two isolates were both neutralized by 2F5 and 4E10 but were not concordant; the ranges in 4E10 and 2F5 IC50 values for these two isolates were 6.1- and 9.9-fold. The remaining eight isolates were neutralized by 4E10 but not 2F5. Sequence analysis of the discordant pairs (4E10-neutralization sensitive and 2F5-neutralization resistant), identified mutations in the 2F5 binding site (Table 3, Figure 9).

Neut. Sensitivity		Percentage of Isolates with Mutation															
		2F5									4E10						
		2F5	4E10	E	L	D	K	W	A	S	L	W	N	W	F	D	I
-	-	86	0	0	14	0	0	29	0	0	43	0	0	0	71	0	29
-	+	63	0	25	57	0	25	0	0	0	0	0	0	0	63	0	13
+	+	61	0	0	3	0	3	19	0	0	19	0	0	0	26	3	19

Table 3. MPER Sequence variability in 4E10- and 2F5- neutralization sensitive and resistant HIV-1 isolates.

Seven isolates were resistant to 2F5 and 4E10-mediated neutralization. The 2F5 epitopes were intact in all but one isolate; the 4E10 epitopes had a greater percentage of amino acid deviations in the asparagine residue. To determine if these epitopes were accessible on the viral surface, HIV-1 capture assays were performed using 2F5 and 4E10 as targets. Four neutralization-sensitive and four neutralization-resistant isolates, two

each from subtype A and B, were tested for their ability to be bound by 2F5 and 4E10. 4E10, and to a lesser extent 2F5, has been shown to bind to lipids within the viral membrane. Antibody interaction with viral constituents other than gp41 MPER was determined by capture of two viral particles that contain the HIV-1 core but do not contain the HIV-1 envelope proteins gp120 or gp41. One viral particle was pseudotyped with vesicular stomatitis virus envelope (23.5% similarity to HIV-1 reference strain HXBII and does not contain HIV-1 MPER epitope) the other virus-like particles did not contain envelope protein (Bald). Antibody capture of HIV-1 was determined by quantifying the amount of antibody-bound p24 core protein, a standard method for HIV-1 quantitation.

Antibody capture of HIV-1 correlated significantly with the neutralization sensitivity of the HIV-1 isolate to the capture antibody ( $p=0.029$ ) (Figure 10 A and B). Viruses that were neutralization-sensitive were captured; viruses that were neutralization-resistant were not captured. On average 4E10 captured more viral particles than 2F5 and also captured a minimal level of all nonspecific and neutralization-resistant viruses.

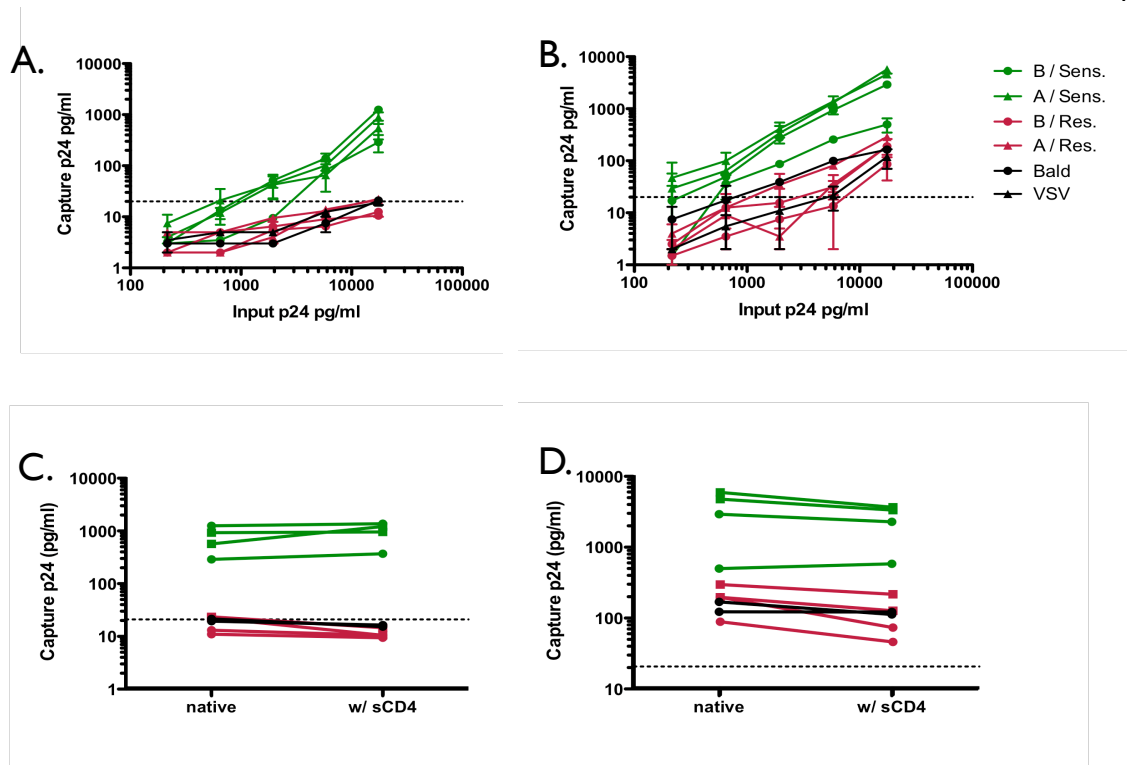


Figure 10. 2F5 (A) and 4E10 (B) capture of HIV-1 isolates and nonspecific viral particles. Effect of sCD4 binding on virus capture by 2F5 (C) and 4E10 (D).

To determine if CD4 binding triggers a conformational change that exposes the MPER epitope, HIV-1 isolates were pre-incubated with soluble CD4 (sCD4) and the capture assays were repeated. For this virus panel, virus capture was not significantly effected by pre-incubation of HIV-1 with sCD4 (Figure 10 C and D). This indicates that neutralization-resistant isolates do not display the MPER epitope in a way that is accessible to antibody binding; this accessibility does not change upon receptor-binding conformational changes within HIV-1 envelope. MPER-directed antibodies are ineffective against these isolates, which represent 12.5% of this panel, from subtypes A, B and D. Alignment of the neutralization-resistant to neutralization-sensitive envelope genes does not provide insight into the inaccessibility of this epitope.

### Characterization of MPER-directed neutralizing activity *in vivo*

MPER-directed neutralizing antibodies elicited during the course of HIV-1 infection were measured. Neutralization breadth and potency of 12 HIV-positive patient plasma samples were assessed against 11 HIV-1 isolates from subtypes A, B and C (Figure 11). Novel HIV-2/HIV-1 chimera viruses were used to assess MPER-specific neutralization. The chimeric viruses contain HIV-2 envelope with HIV-1 MPER. Extensive studies have shown that antibodies that target the HIV-1 envelope do not cross-react with the HIV-2 envelope [66,67,68,75,76]. Only antibodies that interact with HIV-1 MPER should inhibit chimeric viral infection. The parental HIV-2 strain was used as a control to determine background neutralizing activity.

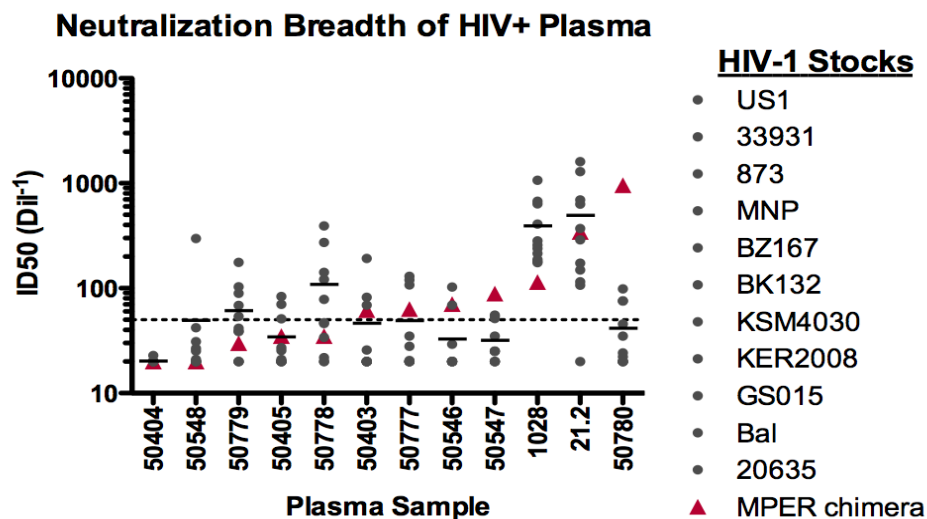


Figure 11: Neutralization profile of 12 HIV-positive plasma samples against 11 HIV-1 isolates from subtype A, B and C. Potency of MPER-directed antibodies measured by HIV-2 env/HIV-1 MPER chimera virus, shown as red triangle.

The HIV-positive plasmas have a range of potency against the MPER-chimeric virus. ID50 values, indicated by red triangles, range from <20 to 959 (Figure 11). 58% of plasmas were able to inhibit of MPER/HIV-2 infection at a dilution greater than 1:50. The 12 plasmas tested did not inhibit infection of the parental HIV-2, indicating the MPER-directed activity was being specifically detected (results not shown). MPER-mediated neutralization does not correlate significantly with the overall neutralization breadth, determined by the percent of HIV-1 isolates neutralized ( $p=0.664$ ), or potency, determined by the average ID50 ( $p=0.491$ ). Individual 50780 has exceptional MPER-specific potency (ID50 = 959) with modest overall neutralization activity (average ID50 = 42).

## **Section 2. bnAb Epitope Reconstruction**

Novel epitopes that bind specifically to MPER bnAbs, 2F5, 4E10 and Z13 were identified. The antibody-epitope interaction was characterized using antibody binding and competition assays.

### **Selection of MPER epitopes**

MPER epitopes were selected by biopanning with phage-displayed peptide libraries against bnAbs 4E10, 2F5 and Z13. Two phage display random peptide libraries were used, Ph.D.12 and Ph.D.c7c, expressing linear dodecapeptides (Ph.D.12) or disulfide-constrained heptapeptides (Ph.D.c7c) fused to the minor coat protein g3p of M13 bacteriophage. Each library contained a complexity on the order of  $10^9$ ; roughly 50 copies of every peptide were included in the initial selection.



Several biopanning strategies were used for peptide selection. 4E10, 2F5 and Z13 were targets for selection of binding phage. 4E10 was further used as a target to select phage-displayed peptide epitopes under competition with HIV-1 or sCD4-bound HIV-1. After three rounds of biopanning the selected phage were enriched in target-specific phage-displayed epitopes, as indicated by the increased recovery (Table 4). Thirty clones from each pool were amplified and screened by ELISA for binding to specific target antibody and nonspecific gp120 antibody, 2G12 (results not shown). M13-displayed epitopes with specific binding two times greater than nonspecific binding were sequenced. Non-repetitive sequences from each pool were aligned using ClustalW; MPER-homologous amino acids are highlighted in red (Table 5).

Target	Library	Selection Condition	Percent Recovery		
			Round 1	Round 2	Round 3
Z13	12	Direct Binding	0.018%	1.000%	5.000%
Z13	c7c	Direct Binding	0.034%	0.014%	0.500%
2F5	12	Direct Binding	0.054%	0.120%	6.200%
2F5	c7c	Direct Binding	0.100%	0.180%	0.260%
4E10	12	Direct Binding	0.026%	0.100%	2.200%
4E10	c7c	Direct Binding	0.016%	0.030%	0.030%
4E10	12	Competition with HIV	0.001%	0.020%	1.850%
4E10	c7c	Competition with HIV	0.002%	0.002%	0.550%
4E10	12	Competition with HIV+sCD4	0.003%	0.011%	0.600%
4E10	c7c	Competition with HIV+sCD4	0.002%	0.005%	1.450%

Table 4: M13 recovery after consecutive rounds of biopanning.

**Target:**  
**Selection:**  
**MPER epitope:**  
**PhD12 Clones:**

2F5  
4E10  
HIV Competition  
HIV+sCD4 Competition

Direct Binding  
Direct Binding  
HIV Competition  
HIV+sCD4 Competition

Direct Binding  
Direct Binding  
HIV Competition  
HIV+sCD4 Competition

Direct Binding  
Direct Binding  
HIV Competition  
HIV+sCD4 Competition

Direct Binding  
Direct Binding  
HIV Competition  
HIV+sCD4 Competition

Direct Binding  
Direct Binding  
HIV Competition  
HIV+sCD4 Competition

Direct Binding  
Direct Binding  
HIV Competition  
HIV+sCD4 Competition

<p>HNQNLDRAII  SEMDDKAKMKI  VELPHDKWHSIT  HDTIPDKAWYA  NVDSGQLDKWAP  SEELDKWYNILT  AMFDKWSHWPT  YSSDKWSWVGTP  GQNFTLTKWTM  DSKDKWALLSHI  NPLTGDKWSWLL  YAPDKWNYLGPA  EVDKAKMTYSS  HNMPDRWSSMH  TSYHQYDKWTTL  SMLSHDKWSGLG  TDTEWDKWSI  NLSLDRWTHITQ  EHTTSFDRWYMI  QPLFDKWPVPR  HLAHDRAWMTG  STSPDKWNTAY</p>	<p>SHTLNFLDLTST  QHWNYFDLSEQQ  GPIIANYSDDTN  RLNDFDLTSVMS  LHAQYNLWDIT  NFLNLSSDITA  LKMFPNMYDLTN  SSNMNTHDITVQ  QSMHWNFSDLTA  MPVSTWNMIDVT  HVPDINWFDYTA  GFTVNMVDITAP  NINHNDVTORLG  NLNYVDMANPR  VINRFNWHDFTT  YYNQNRIDLTVL  NNAKNWTDLTIR  NTAALNHLDLTT  QYHNNVDITKFV  SFNSDSYWDITG  AHYRPFNTIDLT</p>	<p>DMRSIFHDNPFN  NWFNLTQTLMPR  FPSPFEVSNMFH  NWFDCGTTLWHR  SVSVGMPKPSRP  DLQWFDTTMTLW  NWFDCSNEAWNF  VNWWDISSLMRP  EWFDISYSLYRS  NFWDTTTRLTH  NGFDMKTSLLR  KMSNWFELTGL  SWFNLSNTLFKT  NWFDRSHTLFHS  GYWSDYWGMTTH  SHLTSGLPNPVH</p>	<p>TNFFALTEDIYK  EPNFALSMGLQ  DNWFNLTAQWHV  FPSPFEVSNMFH  KMSNWFELTGL  HNWTTSELWR  SSWFDQTYWLYS  SWFDSLNYITPV  DTNWFSTYVMS  TWFDLTHYAWMR  NWFNISTLHYLH  EWFDISYSLYRS  TNFFELTTLKLR  HLNFWDITGELI  NLNWFELTGL  TWFDISSRREL  NWFDCSNEAWNF  NFFMMSYALHTD  ALNVTDRKDTYQ</p>	<p>OSYNWFDHTRWI  NFWELSKYLHMA  TNFFELTTLKLR  LPNWFNLSSNLM  FPSPFEVSNMFH  HGNWFEESSRL  NWFNISTLHYLH  SNWWDLSQMLY  SLQNWFALETDM  NWFEMTLTSSST  SFDFDTLKLHHT  NWFESQSMYTKM  WPSWFDITATA  QNWFGLTSLLSL  KMSNWFELTGL  DNWFNLTAQWHV  NWFDMTLTAYSH  SWFDSLASLTRL  GYDWFDISRHLN  SWFDSLNYITPV</p>
<p>MELDKWA  DKWASFD  DKWAGPN  DKWAFWT  DKWAPNT  DKWAGRW  DKWAGNT  DKWAPAS  DKWAAVT  DKWALAH  DKWAKPF  DKWAHAH  DKWSMAY  PKWTDNS</p>	<p>ALCLGPR  PFGFEIWW  LDGMRSS  LPWEWGD  APWEWGY</p>	<p>MWDIFRN  TLDFIRN  YFDRSS  ERMLFEW  SIFDWPR  YFKTQWG</p>	<p>MWDIFRN  TLDFIRN  YFKTQWG  YFHNQWG</p>	<p>MWDIFRN  TLDFIRN  HLFNWWE  YFHNQWG  LFVWQWG  HPLWQLW</p>

**PhDc7c Clones:**

Table 5: Non-repetitive sequences selected by bnAb biopanning.

### HIV-1 Envelope Sequences

4E10-selected sequences were aligned with alternative HIV-1 epitope sequences previously shown to interact with 4E10, including the gp41 cytoplasmic tail, gp41 fusion peptide and gp120 N-terminal domain. The MPER epitope was the major epitope identified, however several epitopes shared some sequence homology with the alternative envelope sequences, as shown in Figure 12.

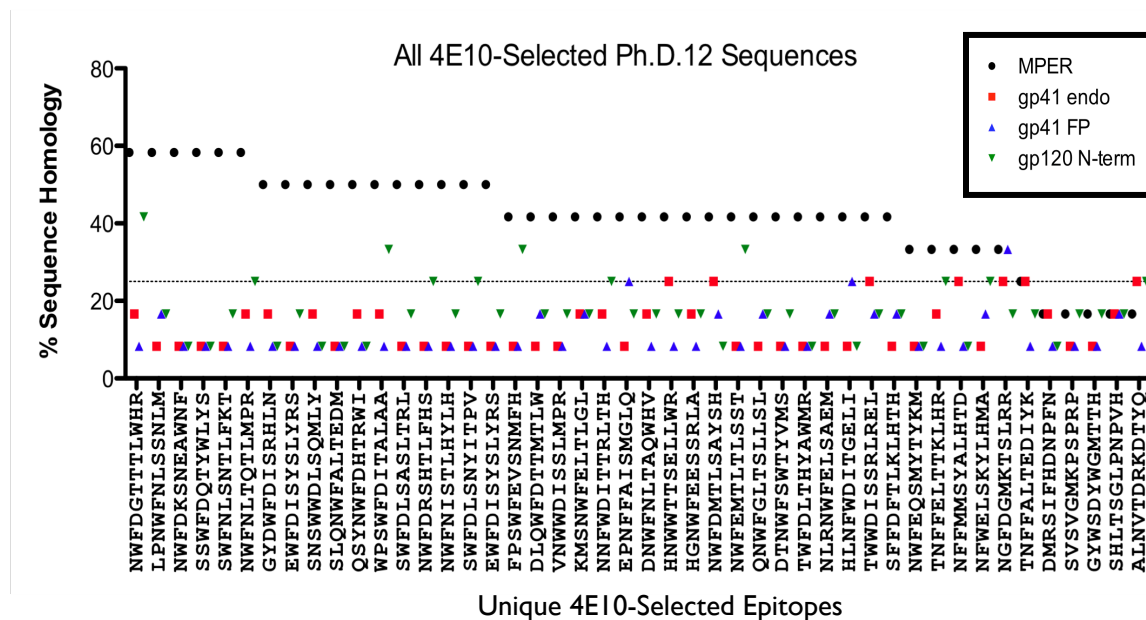


Figure 12: Alignment of 4E10-selected Ph.D.12 sequences with all potential 4E10 HIV-1 binding sites.

### Sequence Analysis of Epitopes Selected by Direct Binding

2F5 and Z13 antibodies strongly selected three amino acid motifs, DKW and NxxDxT, 91% and 98% respectively of the selected M13-dispalyed epitopes including

those amino acids (Figure 13 A). Amino acids outside of the three amino acid motifs were not significantly homologous to the MPER, with on average 21% and 16% sequence homology for 2F5 and Z13 respectively. MPER homologous amino acids include all variants found in the consensus sequences of the major HIV-1 strains. 4E10 antibody selected epitopes with a greater number of MPER homologous amino acids with lower sequence identity. Six amino acids with 50% or greater homology (68% on average) were selected, NWFDxTxxL. The amino acids outside of this core epitope were not significantly homologous to the MPER epitope.

Sequence logos were used to further depict the amino acid conservation pattern of all sequences selected by direct binding to 2F5, Z13 or 4E10 (Figure 13 B). The height of the stack indicates the sequence conservation at that position; the height of the letter reflects the degree of amino acid conservation. Amino acids are colored according to their chemical properties: polar amino acids (G,S,T,Y,C,Q,N) are green, basic (K,R,H) blue, acidic (D,E) red and hydrophobic (A,V,L,I,P,W,F,M) amino acids are black.

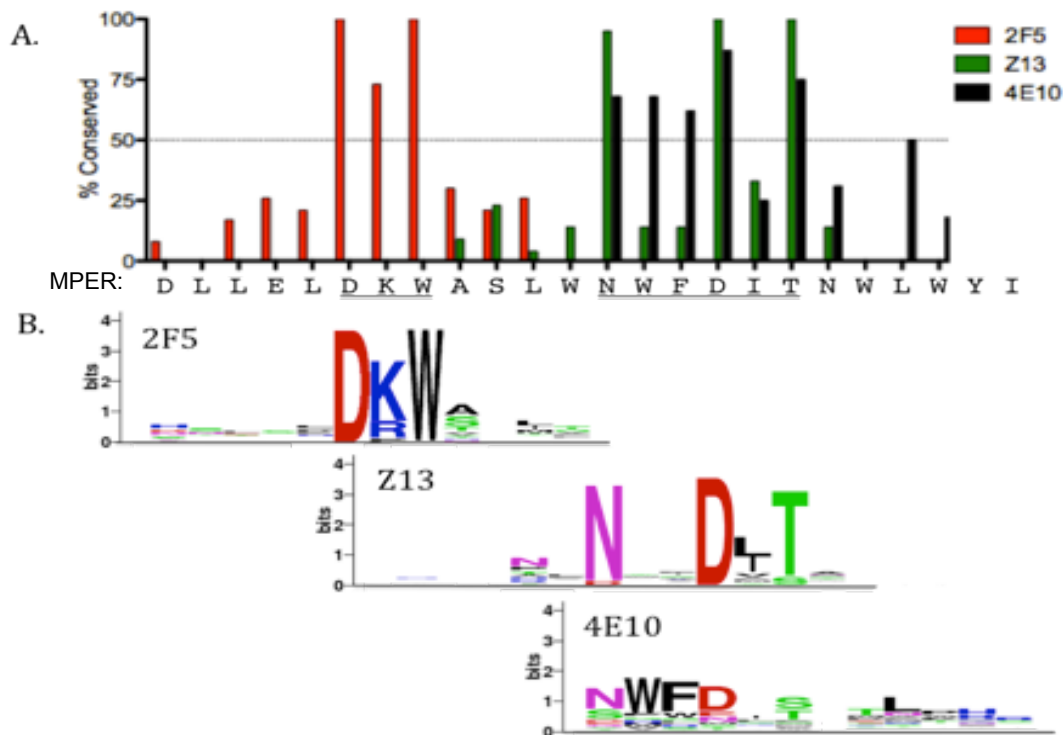


Figure 13: Direct-binding selected epitopes displayed as A) the percentage of all epitopes containing MPER homologous amino acids and B) the amino acid logo of all selected amino acids.

2F5 and Z13 maintain a minimal core epitope with most of the selected epitopes including three, four or five MPER homologous amino acids (Figure 14). 4E10 has a larger epitope, with the majority of selected epitopes including five, six or seven MPER homologous amino acids. While 4E10 appears to require more amino acids for efficient epitope binding, 25% of the selected epitopes contained only two MPER homologous amino acids. These M13-displayed epitopes appear distinct from the native HIV-1 MPER epitope and are therefore considered unique. Unique sequences were subjected to BLAST analysis to identify potential alternative viral or cellular proteins with which the epitopes might correspond. These epitopes did not correspond to any conserved sequence and are

thought to mimic a structural motif to which 4E10 binds. For this comparison the disulfide-constrained heptapeptide epitopes were excluded as they are less likely to represent the linear amino acid sequence than structural binding motifs.

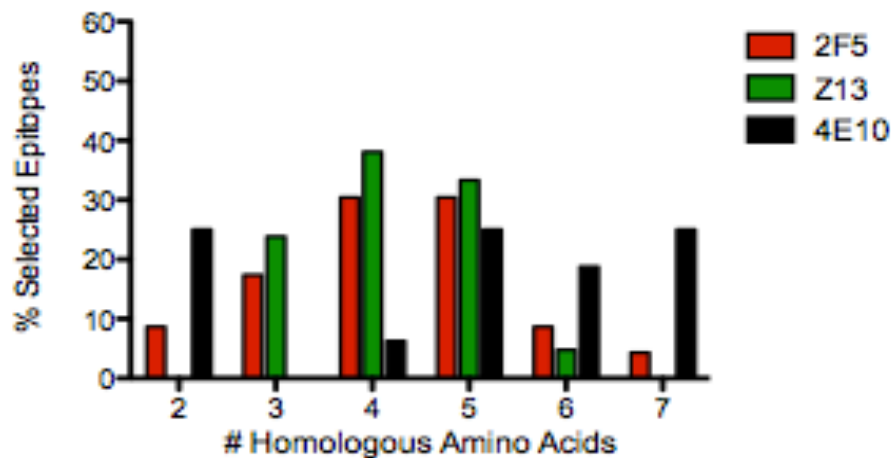


Figure 14: Number of MPER homologous amino acids per selected epitope.

Analysis of the selected epitopes did not identify conserved motifs other than the core epitopes of the respective target bnAb. A unique M13-displayed 4E10 epitope, 12B2 with sequence SVSVG MKPSPR, was previously identified by two independent research groups biopanning against two unrelated targets, a cerebrospinal fluid antibody from a patient with neurocysticercosis [77] and a mouse monoclonal antibody specific for meningococcal lipo-oligosaccharide [78].

### The effect of competition on epitope selection

Epitopes selected by 4E10 in the presence of HIV-1 or sCD4-bound HIV-1 were compared to those selected by direct binding to determine the effect of competition on biopanning. Competition increased selection of the core amino acids, NWFxxT, while

decreased selection of asparagine within the core (Figure 15 A). Competition also increased the number of homologous amino acids present in each selected epitope (Figure 15 B). Epitopes selected in the presence of sCD4-bound HIV-1 contained a minimum of four core MPER amino acids; unique sequences were not selected.

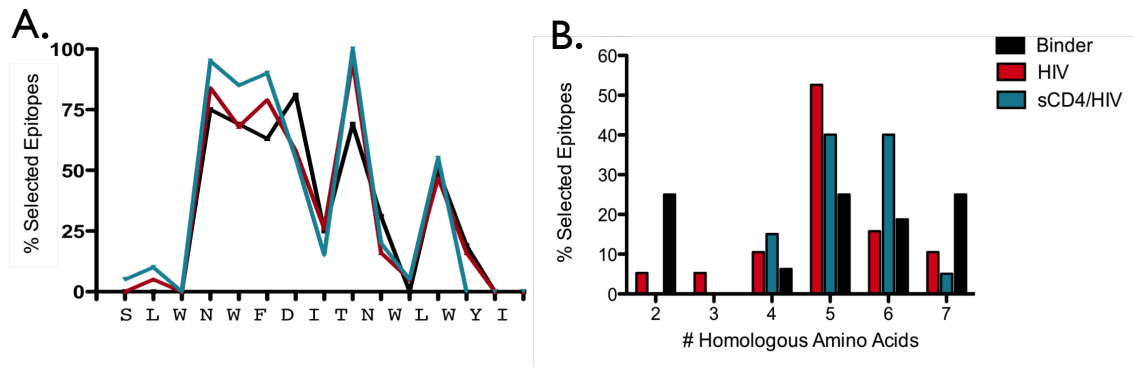


Figure 15: Effect of competition on 4E10 epitope selection. A) MPER homology by amino acid. B) Number of homologous amino acids.

### Relative affinity of M13-displayed epitopes for target antibody

A subset of the select, high-binding or unique M13-displayed epitopes were expanded in large volume and PEG-purified for further characterization (Table 6). 4E10 shows more variability in epitope recognition than 2F5 or Z13, therefore a larger number of epitope variants were selected for analysis. Relative affinity and specificity of each M13-displayed epitope was determined by ELISA titration using target antibody 4E10, 2F5 or Z13, and nonspecific gp120 antibody, 2G12. Reported values are the average of three independent experiments. M13-displayed epitopes bound with varying titers to the target antibody, ranging from  $1.7 \times 10^6$  to  $2.3 \times 10^8$  M13/ml for 4E10,  $6.9 \times 10^6$  to  $2.9 \times 10^8$  M13/ml for 2F5 and  $1.3 \times 10^6$  to  $9.5 \times 10^6$  M13/ml for Z13 (Figure 16 A, B and C). Epitopes did not bind significantly to 2G12, binding titers were  $>2.5 \times 10^9$  M13/ml (data not

shown). Control M13, which does not contain HIV-1 related insert sequence, did not bind to the antibodies. Endpoint binding titers were determined (Figure 16 D).

Target Ab	Library	Condition	Clone#	Sequence
4E10	c7c	Binder	1	SIFDWPR
4E10	c7c	Binder	2	ERMLFEW
4E10	c7c	Binder	3	TLDIRFN
4E10	c7c	Binder	4	YFFDRSS
4E10	12	Binder	1	NWFNLQTLMPR
4E10	12	Binder	2	SVSVGMKPSRP
4E10	12	Binder	3	NWFDRSHTLFHS
4E10	12	Binder	4	NWFDGTTTLWHR
4E10	12	Binder	6	DMRSIFHDNPFN
4E10	12	Binder	7	GYWSDYWGMTTH
4E10	12	HIV+sCD4	1	QSYNWFDHTRWI
4E10	12	HIV+sCD4	2	NFWELSKYLHMA
4E10	12	HIV+sCD4	3	TNFFELTTKLHR
4E10	12	HIV+sCD4	4	LPNWFNLSSNLM
2F5	c7c	Binder	1	MELDKWA
2F5	c7c	Binder	2	DKWASFD
2F5	12	Binder	1	HNSQNLDRWAI
2F5	12	Binder	2	SEMDDKWAKMKI
2F5	12	Binder	3	SEELDKWYNTLT
Z13	c7c	Binder	1	ALCLGPR
Z13	c7c	Binder	2	PFGFELW
Z13	12	Binder	1	SHTLNFLDLTST
Z13	12	Binder	2	QHWNYFDLSEQQ
Z13	12	Binder	3	GPILANYSBITN

Table 6: M13-displayed epitopes selected for further analysis.



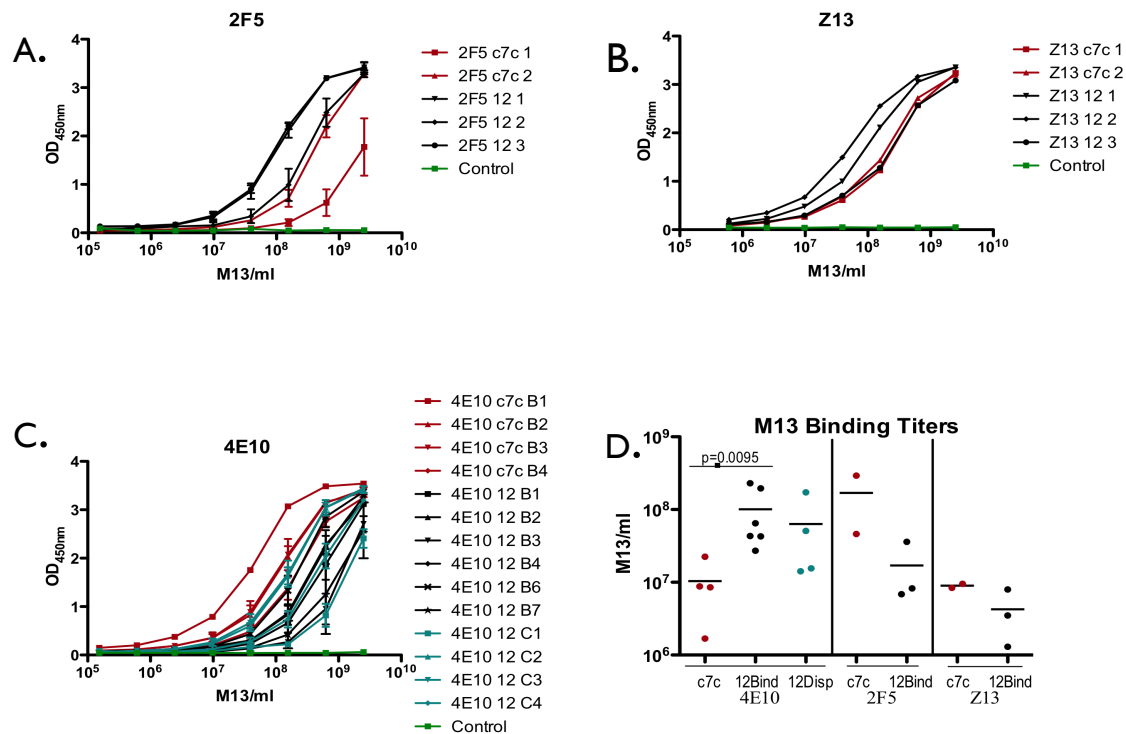


Figure 16: ELISA binding curves for A) 2F5, B) Z13 and C) 4E10 M13-displayed epitopes against the respective target antibody. D) Calculated binding titers.

2F5 and Z13 bound linear dodecapeptide epitopes with higher relative affinity than disulfide-constrained heptapeptide epitopes; the average binding titer was 10- and 2.1-fold lower respectively. 4E10 showed the opposite trend, binding linear dodecapeptide epitopes with lower relative affinity than disulfide-constrained heptapeptide epitopes; the average binding titer was 8.3-fold lower. 4E10 binding titers of disulfide constrained epitopes were significantly higher than linear epitopes selected by direct binding ( $p=0.0095$ ). Epitopes selected by direct binding were compared to those selected under competition with sCD4-bound HIV-1. On average the epitopes selected under competition had a 1.6-fold lower 4E10 binding titers.

**Peptide competition of M13-displayed epitope antibody binding**

The M13 binding ELISA was modified to include peptide competition using MPER (LELDKWASLWNWFNITNWLWYIK) and scrambled nonspecific (LSINEAFKWLDWWTLNDLWYIWK) peptides. Peptide IC<sub>50</sub>s were calculated for each M13-displayed epitope. MPER peptide was able to compete for 2F5 epitope binding, however the same peptide was not able to compete for binding with Z13 epitopes (Figure 17). The average 2F5 IC<sub>50</sub> value was significantly lower than the average 4E10 IC<sub>50</sub> value ( $p=0.0014$ ), with no difference between disulfide-constrained and linear epitopes. 4E10 epitopes had a range of sensitivity to MPER peptide competition, with IC<sub>50</sub>s ranging from epitope 12B7 and 12D3 at  $>100\text{ }\mu\text{g/ml}$  to epitope 12B3 at  $2.3\text{ }\mu\text{g/ml}$ . M13-displayed 4E10 epitope binding was not inhibited by peptide containing sequences of alternative epitopes, including gp41 fusion peptide, gp41 cytoplasmic domain and the N-terminal region of gp120 (data not shown). Nonspecific peptide was not able to compete for antibody binding with any of the epitopes, IC<sub>50</sub>  $>100\text{ }\mu\text{g/ml}$  (data not shown).

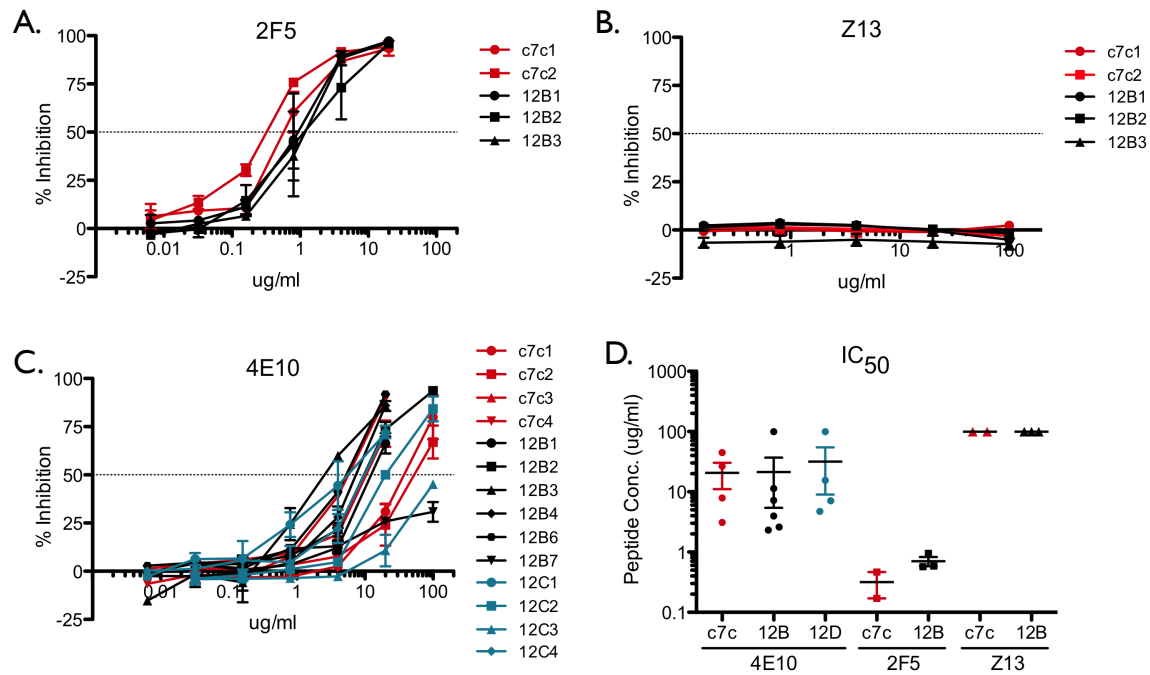


Figure 17. Peptide inhibition curves for A) 2F5, B) Z13 and D) 4E10 along with D) calculated IC<sub>50</sub> values.

### HIV-1 competition of M13-displayed epitope antibody binding

HIV-1 capture assays were used to characterize the M13-displayed MPER epitopes' ability to compete with the native HIV-1 epitope for antibody binding. The HIV-1 isolates used to determine epitope accessibility were tested. Assays were performed using HIV-1 or sCD4-bound HIV-1 as a binding competitor. IC<sub>50</sub>s were calculated and M13-displayed epitopes were stratified by their ability to inhibit HIV capture. A range of competition was observed between HIV-1 and the M13-displayed 4E10 epitopes (Figure 18 A). Several epitopes were able to inhibit capture of all HIV-1 isolates tested while other epitopes were only able to inhibit capture of a few isolates. All M13-displayed 4E10 epitopes were able to compete for capture of VSV-pseudotyped

particles. There was no statistical difference in observed IC<sub>50</sub> between HIV-1 strains tested in this experiment. Several M13-displayed 2F5 epitopes were also able to compete with HIV-1 for antibody binding, however IC<sub>50</sub> values were much higher.

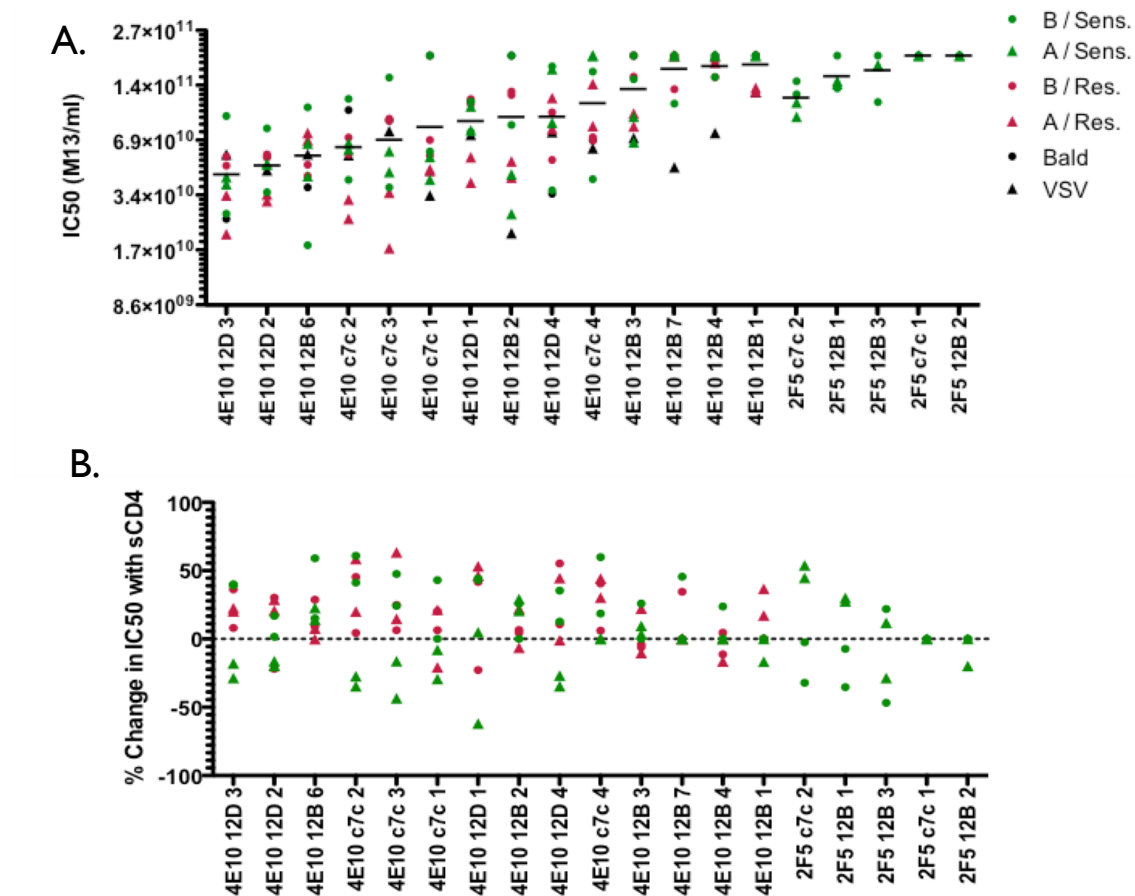


Figure 18: HIV-1 capture competition assay showing A) calculated IC<sub>50</sub>s and B) percent change in IC<sub>50</sub>s when HIV-1 is sCD4-bound.

The effect of HIV-1 sCD4 binding on competition was then determined. Binding competition assays were performed using HIV-1 pre-incubated with sCD4, the percent change in IC<sub>50</sub> was calculated. In general, more M13 was required to achieve the same level of binding inhibition of HIV-1 in the presence of sCD4, shown as a positive percent

change in IC50 value (Figure 18 B). This indicates an increase in relative binding affinity of target antibody for HIV-1 in the sCD4-bound states even though overall level of HIV-1 binding is unaffected. Neutralization-sensitive subtype A HIV-1 isolates behaved significantly differently than other isolates tested ( $p < 0.0001$ ). On average for 4E10, sCD4-bound HIV-1 had lower IC50 values than unbound HIV-1, shown as a negative percent change (Figure 18 B).

M13-displayed epitope characteristics described above, binding titer, and peptide and HIV-1 competition titers, do not correlate with MPER sequence homology or amino acid composition of selected sequence. Relative binding affinity of individual epitopes was predictive of their ability to compete with MPER peptide and HIV-1 for antibody binding (Figure 19).

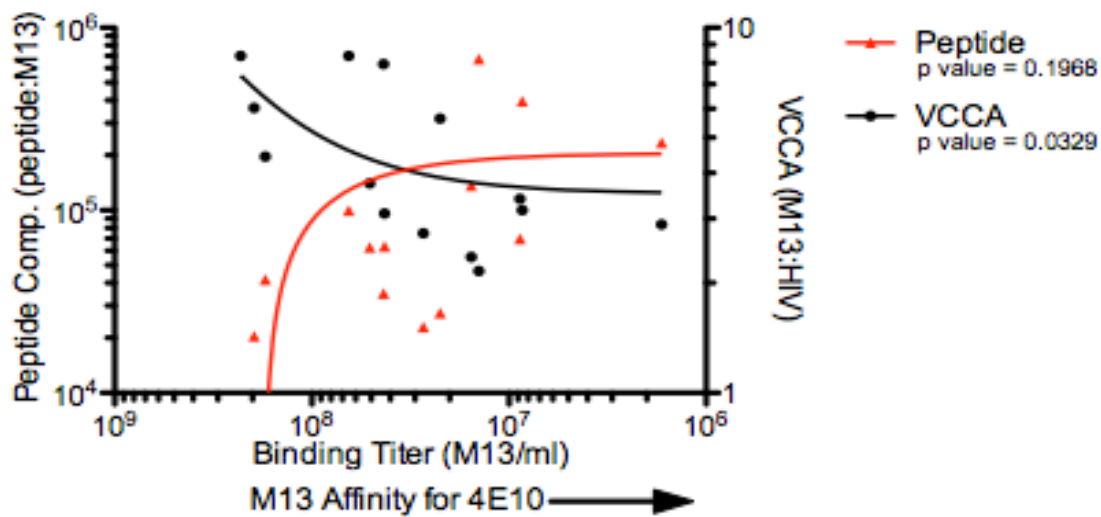


Figure 19: Correlation between relative binding affinity, peptide competition and HIV-1 capture competition of M13-displayed 4E10 epitopes.

**Structural Modeling of M13-displayed epitopes**

Linear M13-displayed 4E10 epitopes were modeled using HHpred and secondary structure was predicted using JPred; epitopes were compared to the predicted structure of the HIV-1 4E10 epitope (Figure 20). The 4E10 epitope is thought to be a helical region containing a hinge [40]. The M13-displayed sequences were predicted to be either helical or unstructured; secondary structure predictions confirmed these results. Five of the ten epitopes are helical or contain helical regions; none of the epitopes align precisely with the 4E10 epitope.





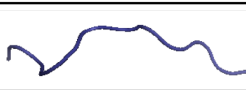
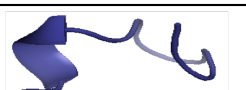
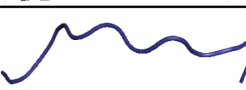
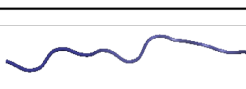

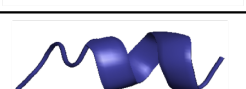
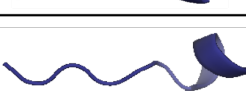
Epitope	Sequence	Structural Model		Secondary Structure
		N-term	C-term	
MPER	LWNWFNITNWLW			HHHHH-HHHHHH
12B1	NWFNLTQTLMPR			----HHHH----
12B2	SVSVGMKPSRP			-----
12B3	NWFDRSHTLFHS			-----
12B4	NWFDGTTTLWHR			-----
12B6	DMRSIFHDNPFN			--HH-----
12B7	GYWSDYWGMTTH			-----
12D1	QSYNWFHDTRWI			-----
12D2	NFWELSKYLHMA			--HHHHH----
12D3	TNFFELTTKLHR			---HHH-----
12D4	LPNWFNLSSNLM			-----HH

Table 7: Structural modeling of linear 4E10 epitopes.

### **Section 3. Analysis of epitope binding in HIV-positive plasma**

In this section, the MPER-specific M13-displayed epitopes were analyzed for their *in vivo* relevance during HIV-1 infection. Epitope-specific antibodies were identified by plasma immunoprecipitation, then neutralization inhibition assays were used to down-select epitopes that were capable of mitigating MPER-specific neutralization.

Plasma reactivity to M13-displayed epitopes was determined by immunoprecipitation of M13 with protein A-immobilized plasma IgG. The panel of HIV-positive plasma samples used to characterize *in vivo* MPER-directed neutralization, was analyzed. Antibody-bound M13 were quantified by western blot using an infrared-labeled secondary antibody. Intensity values were normalized, reported values are the average of two independent endpoints with less than 5-fold difference (Figure 20). Background plasma reactivity for each epitope was determined using normal human plasma, shown as an x. Normal human plasma spiked with 25 µg/ml of 2F5, Z13 or 4E10 was used as a positive binding control, shown in green. Relative intensity units (RIU) less than five were determined to be nonspecific interactions.

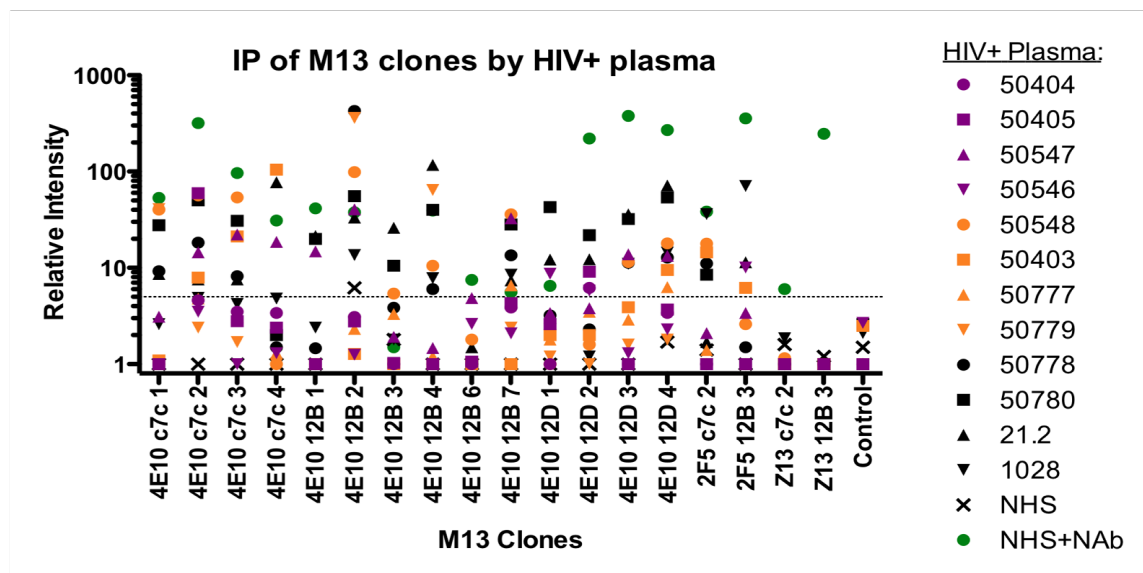


Figure 20: Identification of epitope-specific IgG present in HIV+ plasma samples; immunoprecipitation of M13-displayed epitopes by plasma IgG. HIV-positive plasma are stratified by neutralization potency, from weakly (purple), moderately (orange) to strongly (black) neutralizing.



M13-displayed Z13 epitopes were immunoprecipitated by the positive control but were not recognized by the HIV-positive plasma. M13-displayed 2F5 epitopes were immunoprecipitated by 58% of plasma samples, 42% for the disulfide-constrained epitopes and 33% for the linear epitopes. M13-displayed 4E10 epitopes were immunoprecipitated by 100% of the plasmas tested. Individual epitopes were recognized by a range, from 0 to 67%, of the plasma samples. 4E10 epitope 12B6 was the only epitope not immunoprecipitated by HIV-positive plasma. 4E10 epitope 12B2 had some degree of nonspecific reactivity with plasma, binding to three independent NHS samples with greater than five RIU. 4E10 epitope 12B3 was not immunoprecipitated by the positive control, NHS + 25µg/ml 4E10 (data not shown). 4E10 12B3 and several other M13-displayed epitopes that showed poor immunoprecipitation by the positive control were immunoprecipitated by 4E10 alone at 25ug/ml. Neutralization potency was not directly correlated to the presence of a single M13-displayed epitope.

A trend was found between the number of M13-displayed epitopes recognized by the individual plasma and neutralization breadth and potency (not statistically significant). The greater the number of M13-displayed epitopes bound by plasma IgG, the greater the number of HIV-1 strains neutralized by the corresponding plasma (Figure 21 A). There is also a trend observed between the number of M13-displayed epitopes recognized by the individual plasma and the potency of the anti-MPER response. The greater the number of M13-displayed epitopes bound by plasma IgG, the greater the ID50 value against the HIV-2 env/HIV-1 MPER chimera virus (Figure 21 B). An immune

response that has diversified epitope recognition is more likely to have greater overall neutralization breadth and potency.

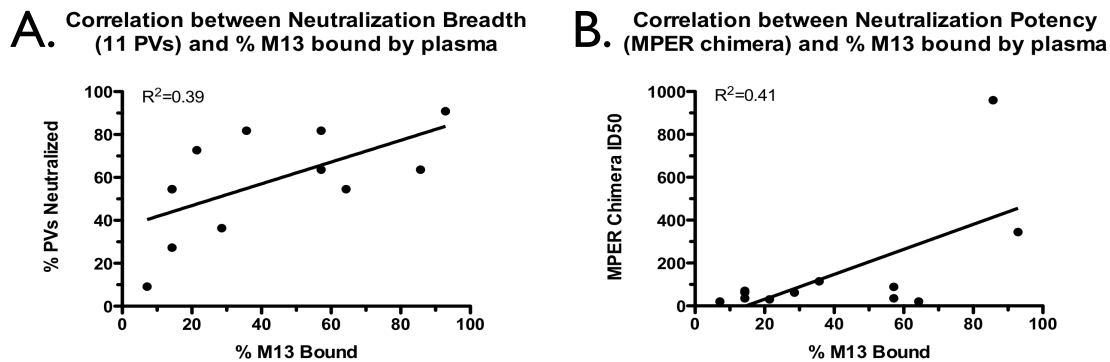


Figure 21. Trend between percent of M13-displayed 4E10 epitopes immunoprecipitated to plasma IgG and A) neutralization breadth and B) epitope-specific neutralization potency of corresponding plasma.

### Analysis of M13 neutralization competition

2F5 and 4E10 M13-displayed epitopes were screened for their ability to reduce plasma-mediated neutralization of HIV-1 MPER. Plasma was diluted to 2xID50 and incubated with a single concentration of M13 before HIV-1 was added. The HIV-2/MPER chimera was used to characterize only MPER-directed neutralization, eliminating neutralization from other antibody specificities. Nine of the twelve plasmas tested neutralized the HIV-2/MPER chimera sufficiently to be used for this analysis. Reported values are the mean of two independent assays. Plasma neutralization inhibited greater than 50% of viral infection; the fold reduction in neutralization mediated by the presence of M13 was determined (Figure 22). Several epitopes, shown on the left were not capable of mitigating neutralization. Antibodies that bind to these specificities may

not recognize the functional HIV-1 envelope. Eight of the M13-displayed epitopes are capable of inhibiting HIV-1 neutralization with a mean fold reduction greater than 1.25.

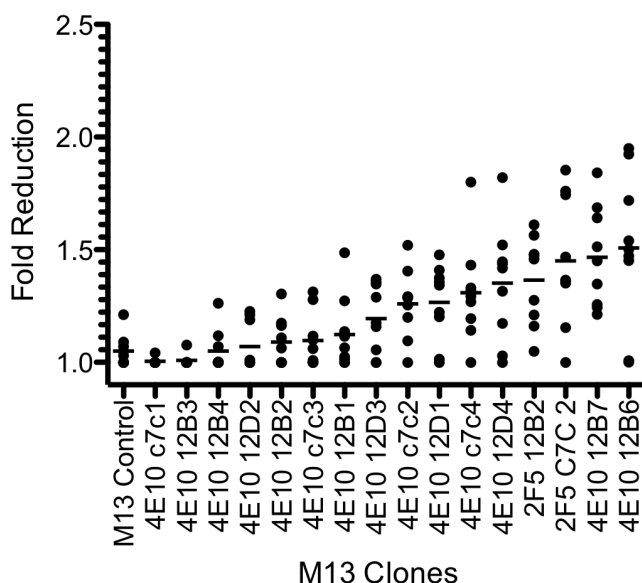


Figure 22: Reduction in plasma neutralization using a single dilution of plasma and M13.

The eight M13-displayed epitopes with the greatest mean fold-reduction in neutralization were further characterized to determine their inhibitory effect on plasma ID50. A single M13 concentration was incubated with a titration of plasma, 2F5 or 4E10, shifts in ID50 or IC50 respectively were determined. MPER peptide and nonspecific, scrambled peptide were used to determine inhibitory effect of peptide on antibody-mediated neutralization. Peptides were added to equal the number of M13 displayed epitopes or to 100-fold excess. The mean of three independent ID50 or IC50 values, standard error and the 95% confidence interval range are shown (Figure 23).

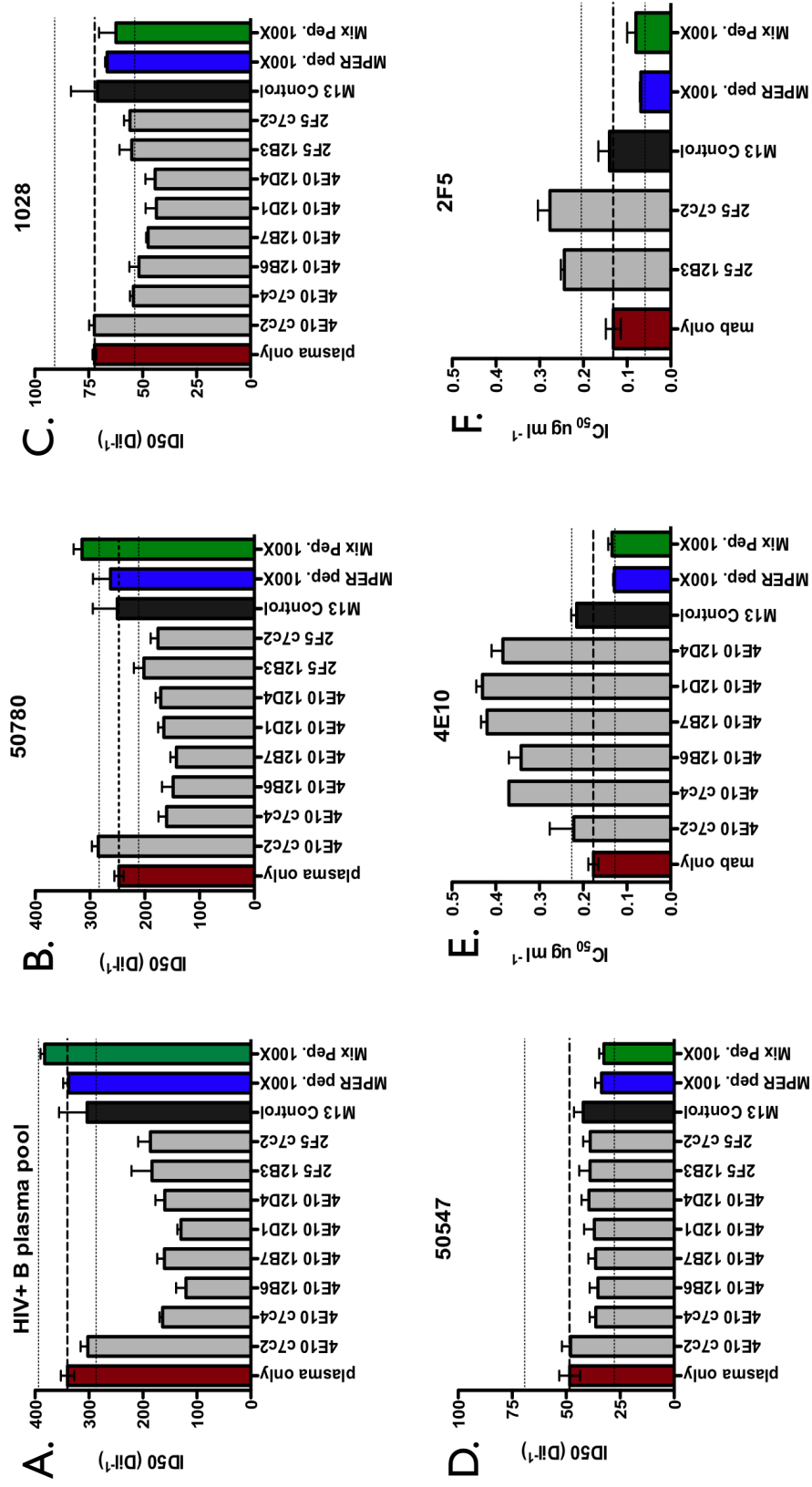


Figure 23: Inhibition of plasma: A) HIV+ B plasma pool, B) 50780, C) 1028 and D) 50547 and bnAb: E) 4E10 and F) 2F5 neutralization by selected M13-displayed epitopes. Thin dashed lines indicate 95% confidence interval around uninhibited neutralization.

Greater inhibition of neutralization was observed in the more potent plasma samples, HIV+ B plasma pool and 50780. Seven of the eight M13-displayed epitopes tested were able to inhibit neutralization of the potently neutralizing HIV-positive B pooled plasma (plasma ID<sub>50</sub> = 340.2). No inhibition of neutralization was observed with the less potent plasma samples 50547 (plasma ID<sub>50</sub> = 48.5). M13-displayed epitopes that are capable of inhibiting plasma ID<sub>50</sub> to a range below the 95% confidence interval are effectively binding to and mitigating the activity of neutralizing antibodies present in the plasma. The five M13-displayed 4E10 epitopes and six M13-displayed 2F5 epitopes that inhibit plasma-mediated neutralization also inhibit neutralization by their respective bnAab. The control M13 did not inhibit neutralization; this indicates that the inhibition is due specifically to the MPER epitope displayed on M13. MPER peptide was also not capable of inhibiting neutralization even when the peptide epitope concentration was 100 times greater than the M13-displayed epitopes concentration.

#### **Section 4. Immunogen Development**

Immunogenicity of the five M13-displayed 4E10 epitopes capable of inhibiting neutralization was evaluated *in vivo*. Thirty-five female BALB/C mice, seven groups of five animals each, were vaccinated with a single M13-displayed epitope, all five M13-displayed epitopes or all five M13-displayed epitopes in combination with HIV-1 gp145 envelope protein (Table 2). The gp145 envelope protein, from an acute clade C HIV-1

infection, has been shown to elicit neutralizing antibodies in rabbits (manuscript in preparation).

### **Analysis of elicited cellular immune response**

Cellular immune responses elicited by vaccination were assessed by INF $\gamma$ -release ELISPOT and intracellular cytokine staining (ICS) assays in both the spleen and lymph node. In these assays HIV-specific responses were measured after stimulation with HIV-1 envelope proteins: gp145, gp140, gp41 or cathepsin degraded gp41. A response two-fold greater than the control group, mice immunized with M13 – no insert, was considered a positive response (Figure 24 and 25). ICS data was analyzed to determine CD3+CD4+ or CD3+CD8+ T-cell specific responses.

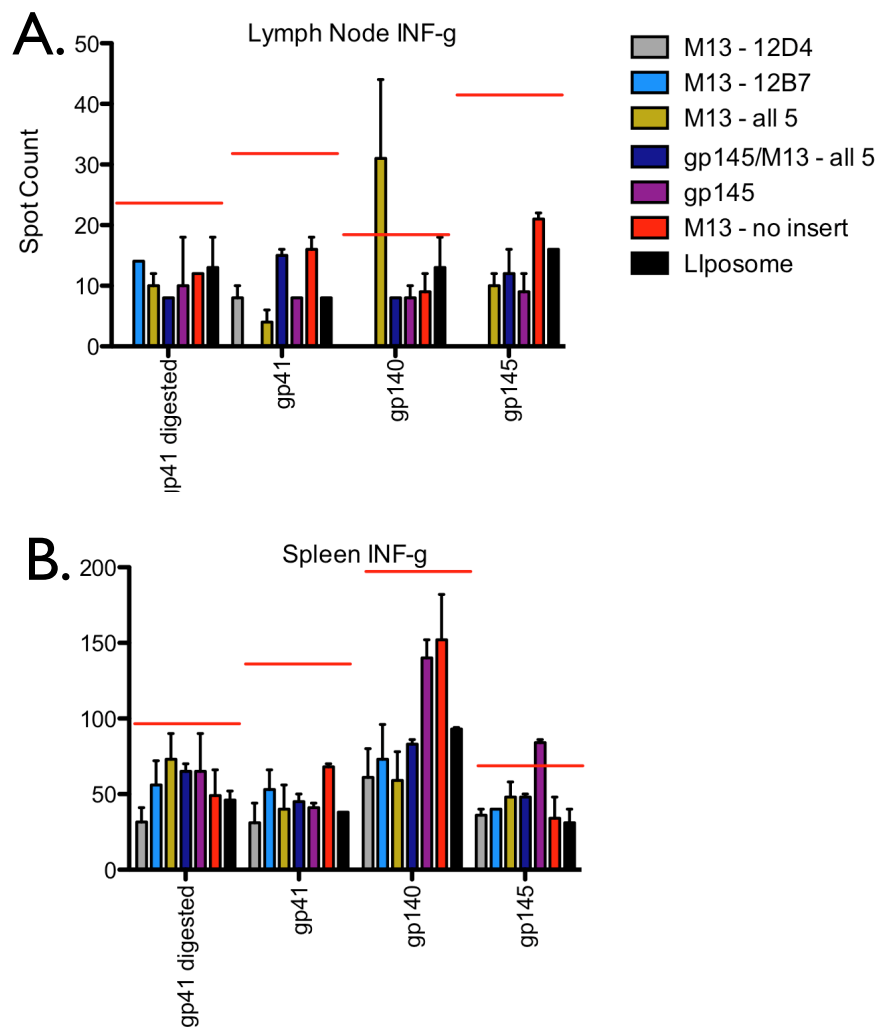


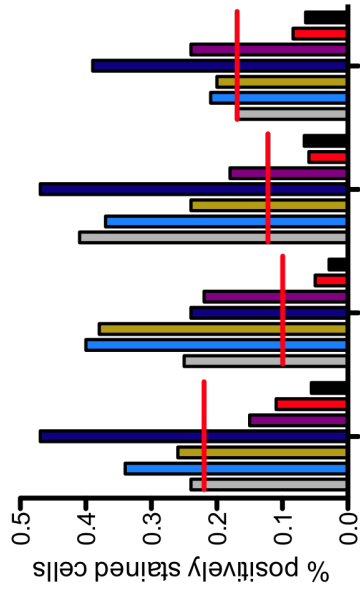
Figure 24: IFN $\gamma$  ELISPOT results in the A) lymph node and B) spleen, shown as spot count after stimulation with HIV-1 antigen.

M13 - 12D4  
 M13 - 12B7  
 M13 - all 5  
 gp145/M13 - all 5  
 gp145  
 M13- No insert  
 Liposome

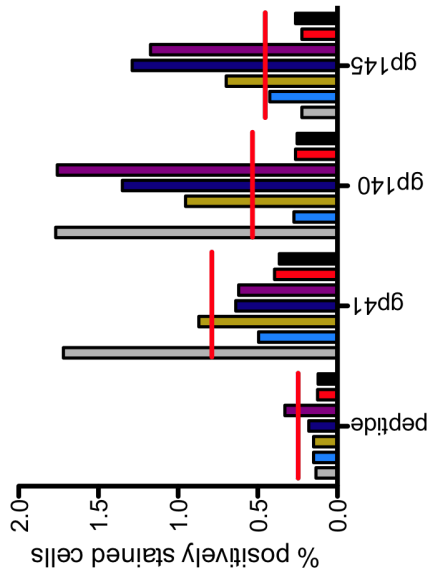
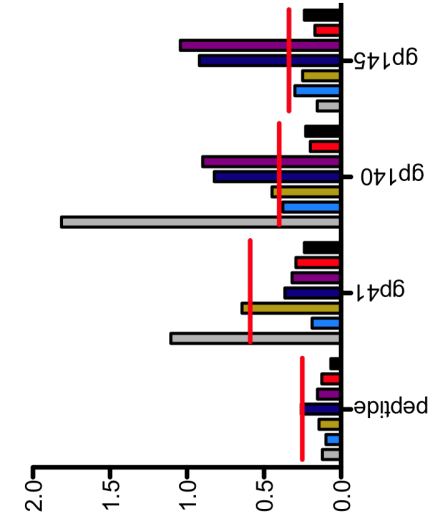
CD3+ CD8+



CD3+ CD4+



Lymph Node



Spleen



Figure 25: Detection of IL-2 expression by intracellular staining.

In the  $\text{INF}\gamma$ -release ELISPOT assay, a single response was observed in all groups in both the lymph node and the spleen; the M13-all 5 immunized group, stimulated with gp140 in the lymph node and the gp145 immunized group, stimulated with gp145 in the spleen (Figure 24). Background responses to gp140 were high in the splenic T-cells. IL-2 responses were observed by ICS for all groups against several HIV-1 envelope antigens;  $\text{TNF}\alpha$ , CD107a and  $\text{INF}\gamma$  responses were not detected. Positive IL-2 responses were more frequent in the lymph node than in the spleen, 85% and 48% positive responses respectively but were lower in magnitude, 3.9-fold and 4.5-fold above control respectively. Positive IL-2 responses were more frequent in the CD4<sup>+</sup> T-cell compartment than in the CD8<sup>+</sup> T-cell. 73% and 60% positive responses respectively and were higher in magnitude, 4.5-fold and 3.8-fold above control respectively (Figure 25). Mice immunized with liposomes only did not have HIV-1 specific cellular responses.

#### **Analysis of elicited humoral immune response**

Humoral immune responses were analyzed by IgG binding ELISA, Biacore and by neutralization assays. Binding titers against gp145 and gp140 were determined for all groups (Figure 26). Animals immunized with gp145 or gp145/M13-all 5 produced antibodies with high titers gp145, average of 512000 and 409600 respectively, and gp41, average of 30400 and 43200 respectively; both groups had the highest titers to the gp145 immunizing protein. The other groups did not have detectable binding titers in this assay with the exception of M13-all 5, which had a weak binding titer to gp145, average 1200.

Biacore was used to characterize epitope-specific IgG binding to MPER peptide in pooled serum; no binding was observed (data not shown).

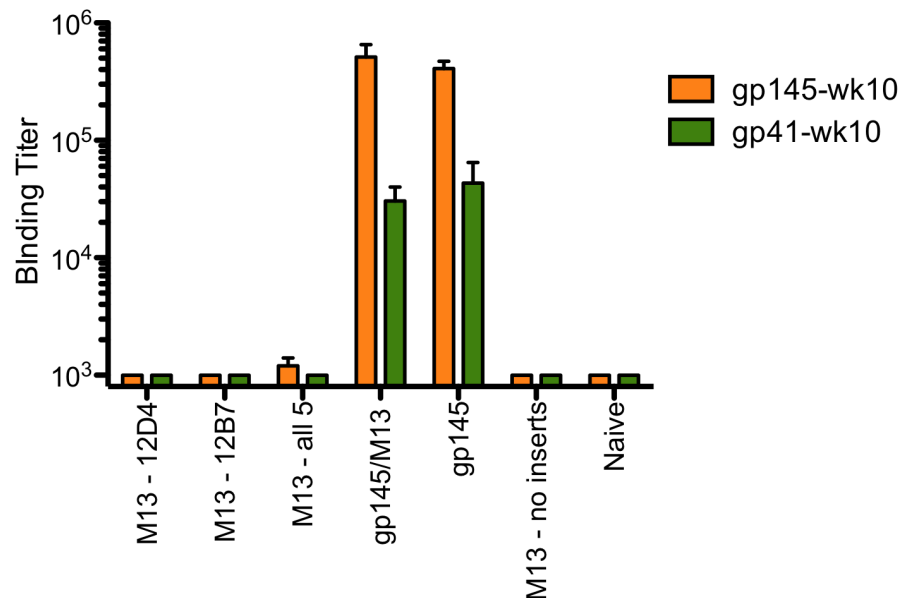


Figure 26: ELISA binding titers of all groups against HIV-1 envelope protein gp145 and gp140.

Neutralization assays were performed using both TZMbl and PBMC as assay targets. Sera were titrated against two neutralization-sensitive HIV-1 strains in both assay platforms and ID50 values were calculated (Figure 27). Animals immunized with gp145/M13-all 5 had the highest neutralization titers in both the TZMbl and PBMC assays, a 2.1- and 1.9-fold increase respectively over the gp145-immunized group. Animals immunized with a single M13-displayed MPER epitope, M13-12D4 and M13-12B7, or multiple M13-displayed MPER epitopes (M13-all 5), also produced HIV-neutralizing antibodies. All sera were screened against the HIV-2/MPER chimera and a

nonspecific viral control, MuLV, no neutralization was observed for either of these viruses.

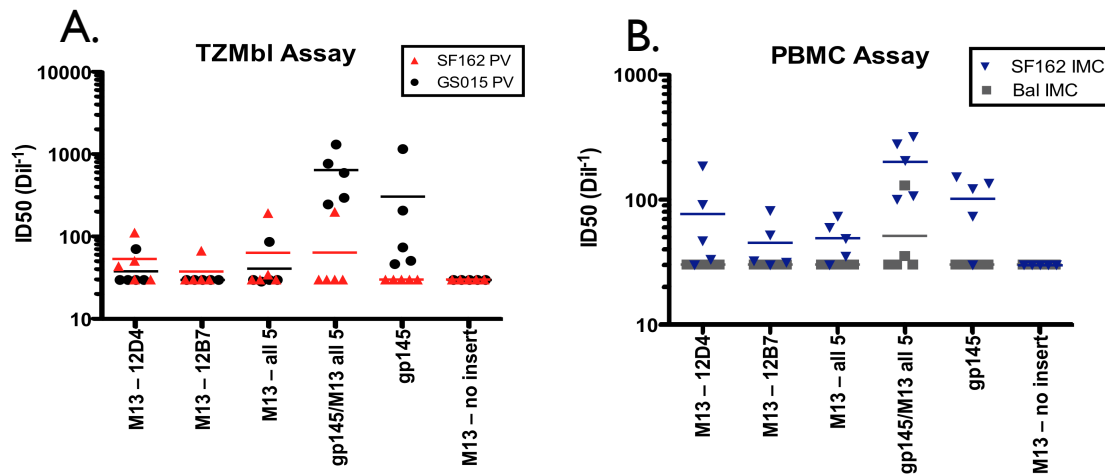


Figure 27: Neutralization results of all groups in two assay platforms, A) TZMbl and B) PBMC.

## Discussion

MPER-specific antibodies, 4E10 and 2F5, neutralize HIV-1 broadly and potently, as shown in figure 8. The neutralization capacity of these two mabs is greater than gp120-specific bnAbs, b12 and 2G12, in agreement with previously published results [35]. MPER-mediated neutralization is observed against all subtypes of HIV-1; this region is critical for efficient viral infection and is therefore highly conserved among diverse isolates [40].

There is debate in the field regarding the timing of MPER epitope exposure on HIV-1. Current models suggest CD4 receptor binding is necessary for full MPER epitope formation, requiring antibody to bind during the transient transitional state immediately before fusion [79,80,81]. In contrast to this model, we found MPER to be exposed on the surface of neutralization-sensitive HIV-1 isolates in both the native and sCD4-bound states, as shown in figure 10 C and D. MPER bnAbs did not bind neutralization-resistant HIV-1 isolates. However, antibody-binding affinity may differ between native and sCD4-bound states, as M13-displayed MPER epitopes were less able to compete for antibody binding with HIV-1 in the sCD4-bound state, figure 18 B.

Antibody binding to MPER relates directly to neutralization profile, shown as a correlation between virus capture and neutralization by MPER bnAbs in figure 10 A and B. This is consistent with the recent observation of Chakrabarti, et al where in antibody-virus “washout experiments” MPER was found to be accessible for antibody binding in the native state of neutralization-sensitive but not neutralization-resistant HIV-1 isolates [82]. Conformational changes induced by receptor binding may improve MPER

accessibility [82,83], however MPER may not be available for antibody binding in neutralization-resistant isolates due of steric occlusion of the epitope [82] or because of epitope mutation [84,85]. In this study, MPER bnAb-resistant isolates were found to have a higher probability of MPER mutation than neutralization-sensitive isolates, shown in table 3 and figure 9. However, mutation studies, where the MPER of neutralization-sensitive isolates are mutated to a neutralization-resistant genotype, were not performed to confirm this observation.

4E10 has previously been shown to interact with HIV-1 envelope regions outside of the MPER [11,46], with membrane-associated lipids [86,87] and host cell proteins [41,87]. Virus capture assays confirm the interaction of 4E10 with non-envelope molecules, seen as capture of VSV-pseudotyped, bald and neutralization-resistant viral particles in figure 10. 2F5, which may have less lipid reactivity [86], does not bind these viral particles. The flexibility of 4E10 epitope recognition may contribute to its broad and potent neutralizing activity.

Biopanning study results confirm the binding promiscuity of 4E10; this bnAb selected forty-six non-repetitive linear and ten non-repetitive disulfide-constrained epitopes, as shown in table 5. 4E10-selected epitopes were significantly more varied than 2F5- and Z13-selected epitopes, which always contained the known core amino acids, figure 13. Several 4E10-selected epitope sequences had minimal sequence homology to MPER, including one epitope (12B2) that was previously identified by two independent groups using two unrelated targets [77,78,88]. Competition with HIV-1 or sCD4-bound HIV-1 drove the selection of epitopes with greater MPER homology. This biopanning

approach allowed for identification of a large number of MPER variants that bind specifically to the target MPER bnAb. The characterization of these epitope variants may provide greater insight into the binding and function of 4E10 than use of gp41 or native MPER peptide alone.

4E10-selected epitopes bound specifically to target bnAb and with few exceptions, binding was inhibited by MPER peptide and native HIV-1, shown in figures 17 and 18. BnAb binding of 2F5-selected epitopes were potently inhibited by linear MPER peptide while Z13-selected epitopes were not. Peptides representing alternative binding epitopes could not inhibit M13-displayed 4E10 epitope binding, indicating that the epitopes and peptides bound to distinct sites on the antibody or the peptides did not bind to 4E10 at all. It is possible that the non-homologous 4E10 epitopes represent unknown binding partners with binding sites that overlap the MPER binding site or represent a structural conformation of MPER.

M13-displayed epitopes were found to bind target bnAbs with varying relative affinities, with significant differences between linear and disulfide-constrained conformations, figure 16. For 4E10, binding titers of disulfide-constrained epitopes were found to be lower than titers of linear epitopes; the reverse was found for 2F5 and Z13. It has been previously suggested that upon binding MPER bnAbs modify the native MPER structure; 4E10 extracts the MPER epitope at a hinge region from the lipid bilayer, 2F5 bind and reorients the N-terminal region and Z13 has little effect on native MPER structure [39,89]. The variation in binding titers may be reflective of the increased relative affinity for the antibody-bound structure of MPER.

Linear 4E10-selected epitopes were modeled to further understand the possible protein structures bound by 4E10, table 7. A crystal structure is available for M13 g3p protein, however the structure does not include the N-terminal region within which the epitopes are inserted. The best model was predicted based on structural elements of homologous proteins. Five out of the ten modeled epitopes were either helical or contained helical regions; the remaining epitopes were unstructured. Of the five helical epitopes only one had little sequence identity to the MPER region. None of the epitopes fully aligned with previously predicted MPER structures. It is possible that antibody binding to M13-displayed epitopes imposes additional structural changes not predicted here. The predicted epitope structure in the M13 g3p protein provides some insight into the MPER conformation recognized by 4E10. The variation in predicted structure gives further evidence to the binding flexibility of this antibody. The structure imposed by the M13 g3p on the bnAb-selected epitopes was required for antibody binding, as epitopes produced as linear or disulfide-constrained peptides were unable to bind to the target bnAb (data not shown).

4E10 is a unique antibody that recognizes a broad range of epitope variants. MPER-specific antibodies develop during HIV-1 infection but they are rarely neutralizing [66]. Previous studies analyzing the humoral response to MPER have used gp41 protein [90], linear MPER peptide [91,92,93,94,95], or chimeric viruses [66] for IgG characterization. In these studies, MPER is represented as the native epitope sequence or alanine-scanning is used to identify critical amino acids within gp41. In this

study, we explored the diversity of response to MPER using the bnAb-selected epitopes.

This allowed us to tease the humoral response to MPER into smaller specificities.

HIV-1 infected individuals were found to generate unique MPER antibodies that bind to a range of epitope variants with specificities that overlap but are distinct from that of 4E10 and 2F5, as shown in figure 20. 4E10- and 2F5-like antibodies were found in 100 and 55% of tested individuals, respectively. Z13-like antibodies were not identified. 4E10 epitope variants bound by HIV-positive plasma included non-homologous 4E10 epitopes indicating these epitopes represent a form of viral structure.

Over the course of HIV-1 infection MPER is presented in several structural states from native state, fusion-intermediates to post-fusion forms. Antibodies are elicited against the different MPER structures however not all antibodies are neutralizing. The majority of these antibodies target the post-fusion form of gp41 MPER, not the pre-fusion or neutralization-competent structures, and will not be protective against infection [21]. In this study, HIV-positive plasma was used to identify MPER variants that represent the neutralization-competent structure. Five 4E10-selected variants were capable of absorbing MPER-specific neutralizing antibodies in HIV-positive plasma, as shown in figure 23.

M13-displayed 4E10 epitopes capable of inhibition neutralization varied in amino acid composition, length and MPER homology. Two M13-displayed epitopes contained the entire linear 4E10-binding site containing six (12D1) or nine (12D4) MPER-homologous amino acids. Two linear M13-displayed epitopes were unique sequences each having only two MPER-homologous amino acids (12B6 and 12B7). One M13-displayed



epitope was disulfide-constrained and did not share linear sequence homology. Epitope sequence and predicted structure were not predictive of neutralization-inhibitory capacity. Additional studies would need to be performed to further characterize the unique structural properties of these M13-displayed MPER epitopes.

Neutralization-competent MPER epitopes elicited HIV-specific immune responses in mice. Cellular immune responses were observed in all groups immunized with M13-displayed 4E10 epitopes or gp145 or both, shown in figures 24 and 25. IL-2 production was detected by intracellular cytokine staining (ICS); IL-2 stimulates proliferation of responsive T-cells. INF $\gamma$  production was not detected by ELISPOT, with the exception of one group against one antigen, or by ICS; TNF- $\alpha$  and CD107a were also not detected by ICS. The elicited cellular immune response was limited as only one immune mediator was detectable. Balb/c mice are known to preferentially develop T helper cell type 2 responses, which favor humoral immune responses over cellular immune responses [96]. Polyspecific cellular immune responses were therefore not expected. Differences in cellular responses were not observed between gp145 and gp145/M13 immunized mice.

Immunization with MPER epitopes in conjunction with gp145 envelope protein boosted the neutralizing antibody response by 2-fold compared to gp145 alone, shown in figure 27. Immunization with M13-displayed 4E10 epitopes alone elicited neutralizing antibodies with low titers. IgG from gp145 immunized groups bound to HIV-1 envelope antigens gp145 and gp41; IgG from M13 (without gp145) immunized animals did not (figure 26). Small sample volumes limited the number of experiments performed in this

immunogenicity study. Additional neutralization assays would be needed to calculate statistical differences between groups.

MPER-specific binding antibodies were not detected in any of the immunized mouse serum. Several methods were used to characterize the MPER-IgG response (data not shown). MPER peptide was used to detect binding antibody in a standard ELISA format as well as by surface plasmon resonance measurement by Biacore. Biacore analysis is better suited for use of hydrophobic peptides than standard ELISA however binding IgG was not detected using either method. MPER-specific neutralizing antibodies were assessed using the HIV-1/MPER chimera virus; neutralization was not observed. It is possible that the neutralizing IgG elicited by immunization with M13-displayed 4E10 epitopes do not cross-react with the native peptide or chimeric viral epitope.

Overall this approach was successful at identifying novel MPER epitopes that can elicit and boost HIV-specific humoral and cellular immune responses in mice. In hindsight there are several modifications that I would make to the experimental design to potentially improve the study outcome. Firstly, the M13 random peptide libraries used here display the insert epitopes as fusion proteins within the g3p minor coat protein for which there are five copies per phage. G3p is the most commonly used protein for phage display, however other libraries are available using the M13 g8p or T7 phage, which have a greater number of displayed epitopes per phage. Immunization of mice with a low epitope to phage ratio may have resulted in lower anti-HIV immune responses than if the mice were immunized with a higher epitope to phage ratio.

Initial study plans involved the production of gp41 protein constructs that included the MPER epitopes selected by phage display. Selected epitopes when produced as peptides were no longer able to bind the target antibody, indicating the g3p protein was imposing an epitope structure that was required for binding. Removal of the epitope from the M13 context would alter its immunogenicity; this required us to immunize with M13 directly. An alternative approach to increase HIV-1 epitope copy number while maintaining the imposed epitope structure would be to produce g3p with selected insert sequences as a fusion protein. This approach has been shown to maintain the N-terminal structure of g3p [97], however this was not tested in this study.

Secondly, M13-displayed HIV-1 MPER epitopes were shown to boost the neutralizing antibodies responses 2-fold when used in conjunction with a gp145 protein. Neutralization was HIV-1 specific, however there is some doubt as to the contribution of the M13-displayed epitope in this response. Immunization with gp145 and M13 that does not contain an MPER insert would have been a more appropriate control to confirm the role of the M13-displayed epitopes.

There are many applications of this experimental approach. In this study, MPER bnAbs 4E10, 2F5 and Z13 were used as target antibodies, however other gp41 or gp120 bnAbs could be used. This approach is well-suited for characterization of loop regions such as the V3 or V1/V2 loops of HIV-1 gp120, both regions are critical vaccine targets [98,99]. Pathogens other than HIV-1, perhaps with lower sequence variability, may also be well suited for this approach [100]. Multiple phage-displayed HIV-1 epitopes could also be used as a multivalent vaccine, incorporating both gp120 and gp41 targets. By

targeting several critical HIV-1 regions at once, there's a greater chance of producing a broader protective immune response.

HIV-positive plasma was used to select M13-displayed epitopes that present HIV-1 MPER in a pre-fusion or neutralization-competent structure. However, characterization of the plasma itself provides insight into the variability of the immune response to MPER. Using this approach, research into the *in vivo* response to MPER could be expanded to answer many questions. In this study, chronically, subtype B infected individuals were characterized. Additionally, chronological plasma samples, starting from acute infection, could be studied to identify the initial MPER variants recognized by the immune system and to characterize the diversification of the response over time. Non-subtype B HIV-positive plasma could also be studied to identify epitope-specific differences between subtypes.

This research approach identified novel, neutralization-competent MPER epitope variants that were effective at eliciting and boosting anti-HIV-1 immune responses in mice. Phage-displayed epitopes can rapidly and inexpensively be selected and can provide epitope-specific depth and variation to HIV-1 vaccine designs without requiring modification to major vaccine components.

## **Bibliography:**

1. De Cock KM, Jaffe HW, Curran JW (2011) Reflections on 30 years of AIDS. *Emerg Infect Dis* 17: 1044-1048.
2. UNAIDS (2010) Global Report: UNAIDS Report on the Global AIDS Epidemic: 2010. UN Joint Programme on HIV/AIDS.
3. Padian NS, McCoy SI, Karim SS, Hasen N, Kim J, et al. (2011) HIV prevention transformed: the new prevention research agenda. *Lancet* 378: 269-278.
4. Chhatbar C, Mishra R, Kumar A, Singh SK (2011) HIV vaccine: hopes and hurdles. *Drug Discov Today* 16: 948-956.
5. McElrath MJ, Haynes BF (2010) Induction of immunity to human immunodeficiency virus type-1 by vaccination. *Immunity* 33: 542-554.
6. Kim JH, Rerks-Ngarm S, Excler JL, Michael NL (2010) HIV vaccines: lessons learned and the way forward. *Curr Opin HIV AIDS* 5: 428-434.
7. Voronin Y, Manrique A, Bernstein A (2010) The future of HIV vaccine research and the role of the Global HIV Vaccine Enterprise. *Curr Opin HIV AIDS* 5: 414-420.
8. Ott DE (2008) Cellular proteins detected in HIV-1. *Rev Med Virol* 18: 159-175.
9. Yoon V, Fridkis-Hareli M, Munisamy S, Lee J, Anastasiades D, et al. (2010) The GP120 molecule of HIV-1 and its interaction with T cells. *Curr Med Chem* 17: 741-749.
10. Huarte N, Lorizate M, Perez-Paya E, Nieva JL (2011) Membrane-Transferring Regions of gp41 as Targets for HIV-1 Fusion Inhibition and Viral Neutralization. *Curr Top Med Chem* 11: 2985-2996.

11. Hager-Braun C, Katinger H, Tomer KB (2006) The HIV-neutralizing monoclonal antibody 4E10 recognizes N-terminal sequences on the native antigen. *J Immunol* 176: 7471-7481.
12. Wayne CK, Berkley SF (2010) The renaissance in HIV vaccine development--future directions. *N Engl J Med* 363: e7.
13. Johnson WE, Desrosiers RC (2002) Viral persistence: HIV's strategies of immune system evasion. *Annu Rev Med* 53: 499-518.
14. McBurney SP, Ross TM (2008) Viral sequence diversity: challenges for AIDS vaccine designs. *Expert Rev Vaccines* 7: 1405-1417.
15. Willey S, Aasa-Chapman MM (2008) Humoral immunity to HIV-1: neutralisation and antibody effector functions. *Trends Microbiol* 16: 596-604.
16. Baum LL (2010) Role of humoral immunity in host defense against HIV. *Curr HIV/AIDS Rep* 7: 11-18.
17. Huber M, Trkola A (2007) Humoral immunity to HIV-1: neutralization and beyond. *J Intern Med* 262: 5-25.
18. Pantophlet R, Burton DR (2006) GP120: target for neutralizing HIV-1 antibodies. *Annu Rev Immunol* 24: 739-769.
19. Montero M, van Houten NE, Wang X, Scott JK (2008) The membrane-proximal external region of the human immunodeficiency virus type 1 envelope: dominant site of antibody neutralization and target for vaccine design. *Microbiol Mol Biol Rev* 72: 54-84, table of contents.

20. Crooks ET, Moore PL, Richman D, Robinson J, Crooks JA, et al. (2005) Characterizing anti-HIV monoclonal antibodies and immune sera by defining the mechanism of neutralization. *Hum Antibodies* 14: 101-113.
21. Frey G, Chen J, Rits-Volloch S, Freeman MM, Zolla-Pazner S, et al. (2010) Distinct conformational states of HIV-1 gp41 are recognized by neutralizing and non-neutralizing antibodies. *Nat Struct Mol Biol* 17: 1486-1491.
22. Hessel AJ, Rakasz EG, Tehrani DM, Huber M, Weisgrau KL, et al. (2010) Broadly neutralizing monoclonal antibodies 2F5 and 4E10 directed against the human immunodeficiency virus type 1 gp41 membrane-proximal external region protect against mucosal challenge by simian-human immunodeficiency virus SHIVBa-L. *J Virol* 84: 1302-1313.
23. Zwick MB, Burton DR (2007) HIV-1 neutralization: mechanisms and relevance to vaccine design. *Curr HIV Res* 5: 608-624.
24. Walker LM, Burton DR (2010) Rational antibody-based HIV-1 vaccine design: current approaches and future directions. *Curr Opin Immunol* 22: 358-366.
25. Robb ML (2010) HIV vaccine development: past, present and future. *IDrugs* 13: 852-856.
26. Wijesundara DK, Jackson RJ, Ramshaw IA, Ranasinghe C (2011) Human immunodeficiency virus-1 vaccine design: where do we go now? *Immunol Cell Biol* 89: 367-374.

27. Rerks-Ngarm S, Pitisuttithum P, Nitayaphan S, Kaewkungwal J, Chiu J, et al. (2009) Vaccination with ALVAC and AIDSVAX to prevent HIV-1 infection in Thailand. *N Engl J Med* 361: 2209-2220.
28. Brown BK, Wieczorek L, Sanders-Buell E, Rosa Borges A, Robb ML, et al. (2008) Cross-clade neutralization patterns among HIV-1 strains from the six major clades of the pandemic evaluated and compared in two different models. *Virology* 375: 529-538.
29. Wei X, Decker JM, Wang S, Hui H, Kappes JC, et al. (2003) Antibody neutralization and escape by HIV-1. *Nature* 422: 307-312.
30. Matar G, Besson F (2011) Influence of the lipid composition of biomimetic monolayers on the structure and orientation of the gp41 tryptophan-rich peptide from HIV-1. *Biochim Biophys Acta* 1808: 2534-2543.
31. Liu SQ, Liu SX, Fu YX (2008) Molecular motions of human HIV-1 gp120 envelope glycoproteins. *J Mol Model* 14: 857-870.
32. Pantophlet R (2010) Antibody epitope exposure and neutralization of HIV-1. *Curr Pharm Des* 16: 3729-3743.
33. Dimitrov DS, Willey RL, Martin MA, Blumenthal R (1992) Kinetics of HIV-1 interactions with sCD4 and CD4+ cells: implications for inhibition of virus infection and initial steps of virus entry into cells. *Virology* 187: 398-406.
34. Go EP, Chang Q, Liao HX, Sutherland LL, Alam SM, et al. (2009) Glycosylation site-specific analysis of clade C HIV-1 envelope proteins. *J Proteome Res* 8: 4231-4242.



35. Binley JM, Wrin T, Korber B, Zwick MB, Wang M, et al. (2004) Comprehensive cross-clade neutralization analysis of a panel of anti-human immunodeficiency virus type 1 monoclonal antibodies. *J Virol* 78: 13232-13252.
36. Gallaher WR, Ball JM, Garry RF, Griffin MC, Montelaro RC (1989) A general model for the transmembrane proteins of HIV and other retroviruses. *AIDS Res Hum Retroviruses* 5: 431-440.
37. Schibli DJ, Montelaro RC, Vogel HJ (2001) The membrane-proximal tryptophan-rich region of the HIV glycoprotein, gp41, forms a well-defined helix in dodecylphosphocholine micelles. *Biochemistry* 40: 9570-9578.
38. Ofek G, Tang M, Sambor A, Katinger H, Mascola JR, et al. (2004) Structure and mechanistic analysis of the anti-human immunodeficiency virus type 1 antibody 2F5 in complex with its gp41 epitope. *J Virol* 78: 10724-10737.
39. Song L, Sun ZY, Coleman KE, Zwick MB, Gach JS, et al. (2009) Broadly neutralizing anti-HIV-1 antibodies disrupt a hinge-related function of gp41 at the membrane interface. *Proc Natl Acad Sci U S A* 106: 9057-9062.
40. Sun ZY, Oh KJ, Kim M, Yu J, Brusic V, et al. (2008) HIV-1 broadly neutralizing antibody extracts its epitope from a kinked gp41 ectodomain region on the viral membrane. *Immunity* 28: 52-63.
41. Alam SM, McAdams M, Boren D, Rak M, Searce RM, et al. (2007) The role of antibody polyspecificity and lipid reactivity in binding of broadly neutralizing anti-HIV-1 envelope human monoclonal antibodies 2F5 and 4E10 to glycoprotein 41 membrane proximal envelope epitopes. *J Immunol* 178: 4424-4435.

42. Sanchez-Martinez S, Lorizate M, Katinger H, Kunert R, Nieva JL (2006) Membrane association and epitope recognition by HIV-1 neutralizing anti-gp41 2F5 and 4E10 antibodies. *AIDS Res Hum Retroviruses* 22: 998-1006.
43. Xu H, Song L, Kim M, Holmes MA, Kraft Z, et al. (2010) Interactions between lipids and human anti-HIV antibody 4E10 can be reduced without ablating neutralizing activity. *J Virol* 84: 1076-1088.
44. Zhu P, Liu J, Bess J, Jr., Chertova E, Lifson JD, et al. (2006) Distribution and three-dimensional structure of AIDS virus envelope spikes. *Nature* 441: 847-852.
45. Zwick MB, Labrijn AF, Wang M, Spenlehauer C, Saphire EO, et al. (2001) Broadly neutralizing antibodies targeted to the membrane-proximal external region of human immunodeficiency virus type 1 glycoprotein gp41. *J Virol* 75: 10892-10905.
46. Buchacher A, Predl R, Strutzenberger K, Steinfellner W, Trkola A, et al. (1994) Generation of human monoclonal antibodies against HIV-1 proteins; electrofusion and Epstein-Barr virus transformation for peripheral blood lymphocyte immortalization. *AIDS Res Hum Retroviruses* 10: 359-369.
47. Kunert R, Wolbank S, Stiegler G, Weik R, Katinger H (2004) Characterization of molecular features, antigen-binding, and in vitro properties of IgG and IgM variants of 4E10, an anti-HIV type 1 neutralizing monoclonal antibody. *AIDS Res Hum Retroviruses* 20: 755-762.

48. Cardoso RM, Zwick MB, Stanfield RL, Kunert R, Binley JM, et al. (2005) Broadly neutralizing anti-HIV antibody 4E10 recognizes a helical conformation of a highly conserved fusion-associated motif in gp41. *Immunity* 22: 163-173.
49. Liao M, Lu Y, Xiao Y, Dierich MP, Chen Y (2000) Induction of high level of specific antibody response to the neutralizing epitope ELDKWA on HIV-1 gp41 by peptide-vaccine. *Peptides* 21: 463-468.
50. Decroix N, Hocini H, Quan CP, Bellon B, Kazatchkine MD, et al. (2001) Induction in mucosa of IgG and IgA antibodies against parenterally administered soluble immunogens. *Scand J Immunol* 53: 401-409.
51. Joyce JG, Hurni WM, Bogusky MJ, Garsky VM, Liang X, et al. (2002) Enhancement of alpha -helicity in the HIV-1 inhibitory peptide DP178 leads to an increased affinity for human monoclonal antibody 2F5 but does not elicit neutralizing responses in vitro. Implications for vaccine design. *J Biol Chem* 277: 45811-45820.
52. Matyas GR, Wieczorek L, Beck Z, Ochsenbauer-Jambor C, Kappes JC, et al. (2009) Neutralizing antibodies induced by liposomal HIV-1 glycoprotein 41 peptide simultaneously bind to both the 2F5 or 4E10 epitope and lipid epitopes. *AIDS* 23: 2069-2077.
53. Wang J, Tong P, Lu L, Zhou L, Xu L, et al. (2011) HIV-1 gp41 core with exposed membrane-proximal external region inducing broad HIV-1 neutralizing antibodies. *PLoS One* 6: e18233.

54. Nelson JD, Kinkead H, Brunel FM, Leaman D, Jensen R, et al. (2008) Antibody elicited against the gp41 N-heptad repeat (NHR) coiled-coil can neutralize HIV-1 with modest potency but non-neutralizing antibodies also bind to NHR mimetics. *Virology* 377: 170-183.
55. Kothe DL, Decker JM, Li Y, Weng Z, Bibollet-Ruche F, et al. (2007) Antigenicity and immunogenicity of HIV-1 consensus subtype B envelope glycoproteins. *Virology* 360: 218-234.
56. Wan Y, Wu L, Liu L, Xu J, Liu Y, et al. (2007) Comparison of immunogenicity between codon optimized HIV-1 Thailand subtype B gp140 and gp145 vaccines. *Vaccine* 25: 4949-4959.
57. Liu L, Wan Y, Xu J, Huang X, Wu L, et al. (2007) Immunogenicity comparison between codon optimized HIV-1 CRF BC\_07 gp140 and gp145 vaccines. *AIDS Res Hum Retroviruses* 23: 1396-1404.
58. Coeffier E, Clement JM, Cussac V, Khodaei-Boorane N, Jehanno M, et al. (2000) Antigenicity and immunogenicity of the HIV-1 gp41 epitope ELDKWA inserted into permissive sites of the MalE protein. *Vaccine* 19: 684-693.
59. Ho J, Uger RA, Zwick MB, Luscher MA, Barber BH, et al. (2005) Conformational constraints imposed on a pan-neutralizing HIV-1 antibody epitope result in increased antigenicity but not neutralizing response. *Vaccine* 23: 1559-1573.
60. Liang X, Munshi S, Shendure J, Mark G, 3rd, Davies ME, et al. (1999) Epitope insertion into variable loops of HIV-1 gp120 as a potential means to improve immunogenicity of viral envelope protein. *Vaccine* 17: 2862-2872.

61. Alving CR, Rao M (2008) Lipid A and liposomes containing lipid A as antigens and adjuvants. *Vaccine* 26: 3036-3045.
62. Morris L (2002) Neutralizing antibody responses to HIV-1 infection. *IUBMB Life* 53: 197-199.
63. Tomaras GD, Haynes BF (2009) HIV-1-specific antibody responses during acute and chronic HIV-1 infection. *Curr Opin HIV AIDS* 4: 373-379.
64. Mikell I, Sather DN, Kalams SA, Altfeld M, Alter G, et al. (2011) Characteristics of the earliest cross-neutralizing antibody response to HIV-1. *PLoS Pathog* 7: e1001251.
65. Doria-Rose NA, Klein RM, Daniels MG, O'Dell S, Nason M, et al. (2010) Breadth of human immunodeficiency virus-specific neutralizing activity in sera: clustering analysis and association with clinical variables. *J Virol* 84: 1631-1636.
66. Gray ES, Moore PL, Choge IA, Decker JM, Bibollet-Ruche F, et al. (2007) Neutralizing antibody responses in acute human immunodeficiency virus type 1 subtype C infection. *J Virol* 81: 6187-6196.
67. Binley JM, Lybarger EA, Crooks ET, Seaman MS, Gray E, et al. (2008) Profiling the specificity of neutralizing antibodies in a large panel of plasmas from patients chronically infected with human immunodeficiency virus type 1 subtypes B and C. *J Virol* 82: 11651-11668.
68. Gray ES, Madiga MC, Moore PL, Mlisana K, Abdool Karim SS, et al. (2009) Broad neutralization of human immunodeficiency virus type 1 mediated by plasma

- antibodies against the gp41 membrane proximal external region. *J Virol* 83: 11265-11274.
69. Montefiori DC (2009) Measuring HIV neutralization in a luciferase reporter gene assay. *Methods Mol Biol* 485: 395-405.
70. Brown BK, Darden JM, Tovanabutra S, Oblander T, Frost J, et al. (2005) Biologic and genetic characterization of a panel of 60 human immunodeficiency virus type 1 isolates, representing clades A, B, C, D, CRF01\_AE, and CRF02\_AG, for the development and assessment of candidate vaccines. *J Virol* 79: 6089-6101.
71. Polonis VR, Brown BK, Rosa Borges A, Zolla-Pazner S, Dimitrov DS, et al. (2008) Recent advances in the characterization of HIV-1 neutralization assays for standardized evaluation of the antibody response to infection and vaccination. *Virology* 375: 315-320.
72. NewEnglandBiolabs (2011) Ph.D. Phage Display Libraries, Instruction Manual. In: Biolabs N, editor. 10 ed.
73. Qiagen (2002) Qiaprep M13 Handbook. In: Qiagen, editor. March, 2002 ed.
74. Edmonds TG, Ding H, Yuan X, Wei Q, Smith KS, et al. (2010) Replication competent molecular clones of HIV-1 expressing Renilla luciferase facilitate the analysis of antibody inhibition in PBMC. *Virology* 408: 1-13.
75. Gray ES, Taylor N, Wycuff D, Moore PL, Tomaras GD, et al. (2009) Antibody specificities associated with neutralization breadth in plasma from human immunodeficiency virus type 1 subtype C-infected blood donors. *J Virol* 83: 8925-8937.

76. Tomaras GD, Binley JM, Gray ES, Crooks ET, Osawa K, et al. (2011) Polyclonal B cell responses to conserved neutralization epitopes in a subset of HIV-1-infected individuals. *J Virol* 85: 11502-11519.
77. Manoutcharian K, Sotelo J, Garcia E, Cano A, Gevorkian G (1999) Characterization of cerebrospinal fluid antibody specificities in neurocysticercosis using phage display peptide library. *Clin Immunol* 91: 117-121.
78. Brett PJ, Tiwana H, Feavers IM, Charalambous BM (2002) Characterization of oligopeptides that cross-react with carbohydrate-specific antibodies by real time kinetics, in-solution competition enzyme-linked immunosorbent assay, and immunological analyses. *J Biol Chem* 277: 20468-20476.
79. Dimitrov AS, Jacobs A, Finnegan CM, Stiegler G, Katinger H, et al. (2007) Exposure of the membrane-proximal external region of HIV-1 gp41 in the course of HIV-1 envelope glycoprotein-mediated fusion. *Biochemistry* 46: 1398-1401.
80. Follis KE, Larson SJ, Lu M, Nunberg JH (2002) Genetic evidence that interhelical packing interactions in the gp41 core are critical for transition of the human immunodeficiency virus type 1 envelope glycoprotein to the fusion-active state. *J Virol* 76: 7356-7362.
81. Gallo SA, Finnegan CM, Viard M, Raviv Y, Dimitrov A, et al. (2003) The HIV Env-mediated fusion reaction. *Biochim Biophys Acta* 1614: 36-50.
82. Chakrabarti BK, Walker LM, Guenaga JF, Ghobbeh A, Pognard P, et al. (2011) Direct antibody access to the HIV-1 membrane-proximal external region positively correlates with neutralization sensitivity. *J Virol* 85: 8217-8226.

83. Peachman KK, Wieczorek L, Polonis VR, Alving CR, Rao M (2010) The effect of sCD4 on the binding and accessibility of HIV-1 gp41 MPER epitopes to human monoclonal antibodies. *Virology* 408: 213-223.
84. Nakamura KJ, Gach JS, Jones L, Semrau K, Walter J, et al. (2010) 4E10-resistant HIV-1 isolated from four subjects with rare membrane-proximal external region polymorphisms. *PLoS One* 5: e9786.
85. Gray ES, Moore PL, Bibollet-Ruche F, Li H, Decker JM, et al. (2008) 4E10-resistant variants in a human immunodeficiency virus type 1 subtype C-infected individual with an anti-membrane-proximal external region-neutralizing antibody response. *J Virol* 82: 2367-2375.
86. Matyas GR, Beck Z, Karasavvas N, Alving CR (2009) Lipid binding properties of 4E10, 2F5, and WR304 monoclonal antibodies that neutralize HIV-1. *Biochim Biophys Acta* 1788: 660-665.
87. Haynes BF, Fleming J, St Clair EW, Katinger H, Stiegler G, et al. (2005) Cardiolipin polyspecific autoreactivity in two broadly neutralizing HIV-1 antibodies. *Science* 308: 1906-1908.
88. Menendez A, Scott JK (2005) The nature of target-unrelated peptides recovered in the screening of phage-displayed random peptide libraries with antibodies. *Anal Biochem* 336: 145-157.
89. Franquelim HG, Chiantia S, Veiga AS, Santos NC, Schwille P, et al. (2011) Anti-HIV-1 antibodies 2F5 and 4E10 interact differently with lipids to bind their epitopes. *AIDS* 25: 419-428.



90. Opalka D, Pessi A, Bianchi E, Ciliberto G, Schleif W, et al. (2004) Analysis of the HIV-1 gp41 specific immune response using a multiplexed antibody detection assay. *J Immunol Methods* 287: 49-65.
91. Muhlbacher M, Spruth M, Siegel F, Zangerle R, Dierich MP (1999) Longitudinal study of antibody reactivity against HIV-1 envelope and a peptide representing a conserved site on Gp41 in HIV-1-infected patients. *Immunobiology* 200: 295-305.
92. Srisurapanon S, Louisirirotchanakul S, Sumransurp K, Ratanasrithong M, Chuenchitra T, et al. (2005) Binding antibody to neutralizing epitope gp41 in HIV-1 subtype CRF 01\_AE infection related to stage of disease. *Southeast Asian J Trop Med Public Health* 36: 221-227.
93. Vanini S, Longhi R, Lazzarin A, Vigo E, Siccardi AG, et al. (1993) Discrete regions of HIV-1 gp41 defined by syncytia-inhibiting affinity-purified human antibodies. *AIDS* 7: 167-174.
94. Calarota S, Jansson M, Levi M, Broliden K, Libonatti O, et al. (1996) Immunodominant glycoprotein 41 epitope identified by seroreactivity in HIV type 1-infected individuals. *AIDS Res Hum Retroviruses* 12: 705-713.
95. Ugen KE, Goedert JJ, Boyer J, Refaeli Y, Frank I, et al. (1992) Vertical transmission of human immunodeficiency virus (HIV) infection. Reactivity of maternal sera with glycoprotein 120 and 41 peptides from HIV type 1. *J Clin Invest* 89: 1923-1930.

96. Chen X, Oppenheim JJ, Howard OM (2005) BALB/c mice have more CD4+CD25+ T regulatory cells and show greater susceptibility to suppression of their CD4+CD25- responder T cells than C57BL/6 mice. *J Leukoc Biol* 78: 114-121.
97. Zwick MB, Bonnycastle LL, Noren KA, Venturini S, Leong E, et al. (1998) The maltose-binding protein as a scaffold for monovalent display of peptides derived from phage libraries. *Anal Biochem* 264: 87-97.
98. Cicala C, Arthos J, Fauci AS (2011) HIV-1 envelope, integrins and co-receptor use in mucosal transmission of HIV. *J Transl Med* 9 Suppl 1: S2.
99. Zolla-Pazner S (2005) Improving on nature: focusing the immune response on the V3 loop. *Hum Antibodies* 14: 69-72.
100. Pande J, Szewczyk MM, Grover AK (2010) Phage display: concept, innovations, applications and future. *Biotechnol Adv* 28: 849-858.